UNIVERSITEIT VAN PRETORIA
UNIVERSITY OF PRETORIA
YUNIBESITHI YA PRETORIA

Effect of the cardiac glycoside, digoxin, on neuronal viability, serotonin production and brain development in the embryo.

by

Jacob John van Tonder

Submitted to comply with requirements of the degree:

M.Sc. Anatomy (with specialization in Cell Biology)

in the School of Medicine, Faculty of Health Sciences,

University of Pretoria, Pretoria, South Africa

2007

UNIVERSITEIT VAN PRETORIA
UNIVERSITY OF PRETORIA
YUNIBESITHI YA PRETORIA

Effect of the cardiac glycoside, digoxin, on neuronal viability, serotonin production and brain development in the embryo.

by

Jacob John van Tonder

SUPERVISORS: Prof E Pretorius
Dr MJ Bester
DEPARTMENT: Anatomy
DEGREE: MSc (Anatomy with specialization in Cell Biology)

ABSTRACT

Digoxin has been known as a treatment for chronic heart failure for over 200 years. Its effect on the heart itself has been extensively studied and its inotropic effect well established. The inotropic effect of digoxin is the result of its inhibition of the membrane sodium pump or Na^+/K^+-ATPase, which plays an important role in maintaining the resting membrane potential across the plasma membrane through constantly pumping Na^+ and K^+ across the plasma membrane. Na^+/K^+-ATPase is not found exclusively in heart muscle. It is also found extensively throughout the brain. As digoxin is the drug of choice for pregnant woman with chronic heart failure, this study aimed to examine how digoxin affects brain development and neurons in culture. The well established chicken embryo animal model was used in this study. To probe for deviations from normal brain development, chicken embryos were exposed *in ovo*. Brains were examined using both transmission and scanning electron microscopy. Microscopy indicated significant damage to the neurons, specifically membranes and mitochondria, as well as cellular death by means of aponecrosis. An unexpected result was premature myelinogenesis in the brain. Chick embryo neurons (CEN) were exposed to digoxin *in vitro* and cell viability was assessed by performing crystal violet (CV) assays. Results showed that cell number increased over time. This is however, impossible as CEN are non-dividing cells and results were therefore

interpreted as an increase in protein synthesis over time, correlating with the myelinogenesis results seen with electron microscopy. To assess membrane integrity, fluorescence microscopy was performed using propidium iodide as stain. Results from this experiment showed a sharp increase in propidium iodide uptake in exposed cells indicative of the membrane damage caused by digoxin. These results also correlated with the aponecrosis seen with electron microscopy, as the nuclei indicated apoptosis while propidium iodide is normally only absorbed by cells undergoing necrosis. Finally, a literature search was conducted to shed some light on the role that digoxin plays in serotonin production and levels in the brain. From the literature it seems that digoxin could increase serotonin production and elevate serotonin levels in the brain, which may influence normal brain development and may therefore play a role in myelinogenesis in the brain.

Declaration.

I, Jacob John van Tonder, hereby declare that this research dissertation is my own work and has not been presented for any degree of another University;

Signed……

Date……

Department of Anatomy, Faculty of Health Sciences, School of Medicine,
University of Pretoria,

Pretoria

Acknowledgements.

First, I would like to dedicate this dissertation to both my parents for providing me with this opportunity and for believing in me.

Second, if anyone involved in this study need to be thanked it must certainly be my two supervisors, Prof. R. Pretorius and Dr. M.J. Bester, as well as Me. J. Marx. Without the help and patience of these three persons, I would not have been able to tackle this study.

I would also like to thank Mr. C. vand der Merwe and Mr. A. Hall from the microscopy unit for all their help and advice without which *Chapters 3* and *5* would not have been possible.

Finally, I must thank God. Without Him nothing is possible.

List of Abbreviations, Symbols and Chemical Formulae

AIF	Apoptosis inducing factor
ANOVA	Analysis of variance
ATP	Adenosine triphosphate
BN-PAGE	Blue native polyacrylamide gel electrophoresis
BSA	Bovine serum albumin
Ca^{2+}	Ionised calcium
$CaCl_2$	Calcium chloride
CAM	Chorionic-allantoid membrane
CEN	Chicken embryo neuron(s)
CICR	Calcium-induced calcium release
cm^2	Centimetre square
CO_2	Carbon dioxide
CNS	Central nervous system
CV	Crystal violet
DAPI	4',6-diamidine-2-phenylindole
ddH_2O	Doubly distilled de-ionised water
DHEAS	Dehydroepiandotestoterone sulphate
DLIF	Digoxin-like immunoreactive factor
DMSO	Dimethyl sulphoxide
DNA	Deoxyribonucleic acid
DPBS	Dulbecco's phosphate buffer solution
EM	Electron microscopy
EMEM	Eagle's minimum essential medium
ER	Endoplasmic reticulum
ETC	Electron transport chain
EtOH	Ethanol
FCS	Foetal calf serum
g	Grams
HBSS	Hank's balanced salt solution

HPLC	High-pressure liquid chromatography
HSP	Heat shock protein
I	Independent groups
IP_3	Inositol triphosphate
K^+	Ionised potassium
KCl	Potassium chloride
kDa	Kilodalton
KH_2PO_4	Potassium dihydrogen phosphate
L	Litre
M	Molar
MAO-A	Monoamine oxidase A
MBP	Myelin basic protein
mg	Milligrams
Mg^{2+}	Ionised magnesium
$MgCl_2$	Magnesium chloride
$MgSO_4$	Magnesium sulphate
min	Minutes
mL	Millilitres
MPT	Mitochondrial permeability transition
mRNA	Messenger ribonucleic acid
MTT	3-(4,5-dimethyl-2-thiazolyl)-2,5-diphenyl-3H-tetrazolium bromide
Na^+	Ionised sodium
NaCl	Sodium chloride
ng	Nanograms
$NaHCO_3$	Sodium hydrogen carbonate
Na_2HPO_4	Disodium hydrogen phosphate
NaH_2PO_4	Sodium dihydrogen phosphate
nM	Nanomolar
nm	Nanometres

NR	Neutral red
OsO_4	Osmium tetraoxide
p	Probability
PCV	Percentage of control values
PI	Propidium iodide
PMCA	Plasma membrane calcium-ATPase
PP2B	Protein phosphatase 2B
qk^v	Quakingviable
ROS	Reactive oxygen species
RyR	Ryanodine receptor
SEM	Scanning electron microscope
SERCA	Sarco-endoplasmic reticulum calcium-ATPase
Serotonin	5-hydroxytryptophan
S_{pooled}	Standard deviation across independent groups
SR	Sarcoplasmic reticulum
Src-PTK	*Src* family of protein tyrosine kinases
TEM	Transmission electron microscope
TH	Tryptophan hydroxylase
5-HT	5-hydroxytryptophan (Serotonin)
%	Percentage
α	Alpha
B	Beta
ºC	Degrees celsius
µL	Microlitres
µM	Micromolar
$[X]_e$	Extracellular concentration of X
$[X]_i$	Intracellular concentration of X

SUMMARY:

Effect of the cardiac glycoside, digoxin, on neuronal viability, serotonin production and brain development in the embryo.

Digoxin, a cardiac glycoside, has been used for over 200 years to treat chronic heart failure. Its inotropic effect is established by inhibition of the enzyme Na^+/K^+ ATPase, which results in increased in cytoplasmic calcium. Digoxin is the treatment of choice for pregnant women suffering from chronic heart failure and the effect of digoxin on embryonic brain development was studied. Following *in ovo* exposure, electron microscopy revealed neuronal death by aponecrosis as well as premature myelination in the brain. *In vitro* studies with crystal violet indicated cell death accompanied by an increase in protein synthesis. Studies with propidium iodide, correlated with electron microscopic findings that apoptosis and necrosis occur simultaneously (aponecrosis). A literature review showed that digoxin is capable of increasing brain serotonin levels through increasing tryptophan transport into the brain, increasing the activity and amount of tryptophan hydroxylase and by inhibiting monoamine oxidase A.

Table of contents

List of tables

List of figures

SEM micrograph of control chick embryo brain exposed to 10µL 50% EtOH. Significant damage to the plasma membrane can be seen as the rough appearance of the cell surface. Scale bar in inset = 0.5µm.

TEM micrograph of control chick embryo brain exposed to 5µL 50% EtOH. *N* = nucleus; *No* = nucleolus; *Cyt* = cytoplasm showing swelling. Notice the amount of swelling of the neuronal cytosols (dashed lines), indicative of necrosis. 4 300 × magnification.

TEM micrograph of experimental chick embryo brain exposed to 5µL 50% EtOH. *RER* = rough endoplasmic reticulum; *Mt* = mitochondrium. Reversible mitochondrial damage (arrow). Cellular swelling is visible in the dispersion of cytoplasmic contents (dashed line). 36 000 × magnification.

SEM micrograph of experimental chick embryo brain exposed to 32nM digoxin in 50% EtOH. The neuron has suffered significant membrane damage when examining the surface of the cell body, better seen in the inset. Scale bar of inset = 0.2µm.

SEM micrograph of chick embryo brain not exposed to digoxin or ethanol. Notice the smooth appearance of the surface of the cell body.

TEM micrograph of experimental chick embryo brain exposed to 128nM digoxin in 50% EtOH. *Ax* = axon. Nerve bundle being encapsulated through myelination (arrows). 43 000 × magnification.

Myelinated axon of neuron exposed to 128nM digoxin in 50% EtOH. (A) This SEM micrograph shows the axon extending from the distal neuronal cell body. The arrows indicate the plane between the myelin layer surrounding the exposed axon. (B) More distal shot of the axon in (A) and a higher magnification micrograph. Myelin-covered and exposed areas of the axon is clearly visible in the inset in (B).

TEM micrograph of experimental chick embryo brain exposed to 128nM digoxin in 50% EtOH. *N* = nucleus; *Asterisk* = Glial cell processes acting as support and packing for neural structures. Morphologically brain structure and organization is much more advanced as compared to control brains. 4 300 × magnification.

TEM micrograph of experimental chick embryo brain exposed to 128nM digoxin in 50% EtOH. *Mt* = mitochondrium; *P* = glial cell process; *Asterisk* = outline of a glial cell process. High magnification of a glial cell process. A juxtapositioned cell's plasma membrane is indicated by the arrowheads. Severely damaged mitochondria. 28 000 × magnification.

Diagrammatic illustration pertaining to the hypothesis on how digoxin could increase brain serotonin levels.

Chapter 1:

Introduction

Digoxin has been known as a treatment for chronic heart failure for over 200 years. The effect of this drug on the heart itself has been extensively studied and its inotropic effect well established. In a nutshell, digoxin inhibits a specific ion pump on the cell membrane known as the membrane sodium pump or Na^+/K^+ ATPase, which causes another membrane ion exchanger to reverse its action and increase calcium in the cell. This allows the heart muscle to perform more powerful contractions and in this way increase cardiac output.

Some tissues in the body, such as cardiac and neural tissues, have the ability to conduct electrical impulses in the form of action potentials. Cells are enclosed in plasma membranes that contain channels for ions to allow these to cross the plasma membrane from the extracellular space to the intracellular space and *vise versa*. Ion concentrations across the plasma membrane are closely maintained and this establishes the membrane potential across the plasma membrane between the differing ion concentrations. Once these ion concentrations are disturbed and the resting membrane potential disrupted or depolarized, it results in an action potential, which is simply a continuing depolarization along the plasma membrane. Neuronal tissue utilizes this action potential to convey information throughout the brain as well as to other areas of the body, like skeletal muscle.

Na^+/K^+-ATPase plays an important role in maintaining ion concentrations across the plasma membrane and therefore also maintains the resting membrane

potential. Therefore, if digoxin inhibits Na^+/K^+-ATPase, it should have a profound effect on the resting membrane potential.

Na^+/K^+ ATPase is found widely through the neuronal tissues of the brain. If digoxin then plays such a noticeable and life-saving role in the heart, what effect would this drug have on neuronal tissue, which shares similarities with cardiac tissue with regards to the resting membrane potential and ion gradients? The importance of this question is amplified by the fact that digoxin is the drug of choice in pregnant woman with chronic heart failure, when taken into account that embryonal development is very sensitive to *ex utero* influences such as ethanol, which may result in Foetal Alcohol Syndrome.

In this dissertation I examine the effect that digoxin has on neuronal ultra structure, neuronal viability and finally what effect digoxin could have on brain levels of the neurotransmitter serotonin. In the chapter on ultra structure, I specifically look at membrane integrity and organelle pathology. Neuronal viability is assessed in two separate ways to confirm the results that are obtained and a literature review is conducted to probe for any links that may be present in currently available literature that could direct future research into the effects of digoxin on serotonin production and content within the central nervous system.

The following research questions directed the course of this study:

1. What effect will digoxin, *in ovo*, have on neuronal ultra structure in the chick embryo?
2. How will digoxin influence the viability of chick embryo neurons *in vitro*?
3. Can the results obtained from research question 2 be confirmed?
4. Does any research support an effect that digoxin has or may have on serotonin production, brain serotonin content and if so, how is this effect established?

Chapter 2:

Literature review

2.1. DIGOXIN

2.1.1. Discovery

In 1785, Sir William Withering published his work on the application of the foxglove plant to treat edematous states and chronic heart failure (Withering, 1941). Digitalis preparations have been used, perhaps for as much as a millennium, to treat medical conditions including dropsy (Yusuf, 1993). It's only since the early 20th century that digitalis preparations has been used to treat patients with heart failure and sinus dysrhythm (Yusuf, 1993; Christian, 1922; Marvin, 1927).

2.1.2. Structure

Digoxin forms part of a family of steroidal glycosides dubbed the cardiac glycosides. A few other molecules that are classified as cardiac glycosides include: digitoxin; transvaalin; and ouabain. Cardiac glycosides consist of two parts: a sugar (glycone) and a non-sugar (aglycone), which is a steroid. At the 17th position of the molecular structure is a R-group, which determines the classification of cardiac glycoside as either a cardenolide or bufidienolide. Figure 2.1. shows the structure of digoxin, a cardenolide (Marx *et al.*, 2005).

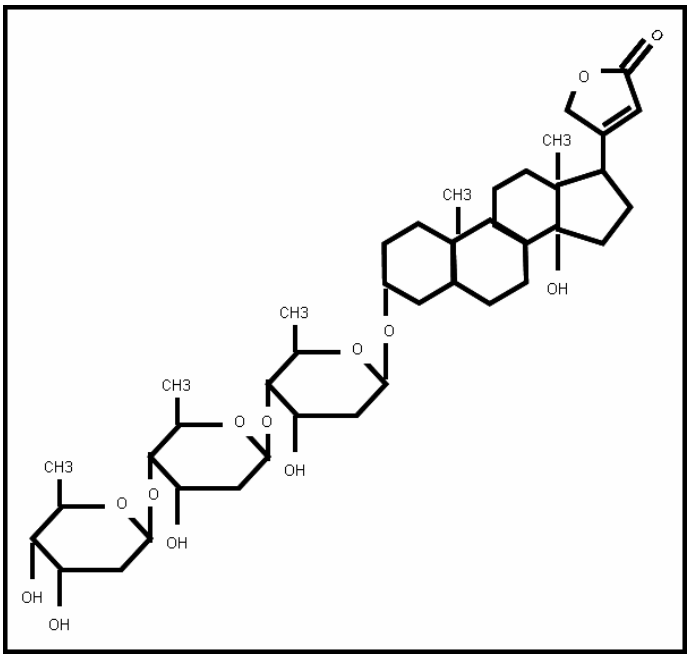

Fig. 2.1. The chemical structure of digoxin

2.1.3. Mechanism of Action

2.1.3.1. Therapeutic doses

The therapeutic index of digoxin is 0.5-2ng/mL (Qasqas *et al.*, 2004; DIG, 1996; Eichhorn and Gheorghiade, 2004; Datta and Dasgupta, 2004). Digoxin binds to the catalytic α-subunits of the Na^+/K^+-ATPase enzyme thereby inhibiting its normal functioning (Marx *et al.*, 2005; Gerbi *et al.*, 1999; Kurup and Kurup, 2002; Reinés *et al.*, 2001). Under normal conditions this enzyme is necessary to exchange extracellular K^+ ($[K^+]_e$) for intracellular Na^+ ($[Na^+]_i$) to maintain the resting membrane potential of the cell (Marx *et al.*, 2005; Kent *et al.*, 2004; Gerbi *et al.*, 1999).

When the enzyme is inhibited, $[Na^+]_i$ is not extruded to the extracellular space, which results in an increase in $[Na^+]_i$. To relieve the excess $[Na^+]_i$ another membrane pump, the Na^+/Ca^{2+} exchanger, which normally exchanges $[Na^+]_e$ for

$[Ca^{2+}]_i$, reverses its action causing an increase in $[Ca^{2+}]_i$ (Marx *et al.*, 2005; Kurup *et al.*, Oct 2002; Hambarchian *et al.*, 2004). High levels of $[Ca^{2+}]_i$ induces the release of Ca^{2+} from the sarcoplasmic reticulum (SR) (Kurup *et al.*, Oct 2002; Huang *et al.*, 2004), resulting in an even greater increase in $[Ca^{2+}]_i$ and it is this increase in $[Ca^{2+}]_i$ that causes the inotropic effect which can be used therapeutically in patients with chronic heart failure.

2.1.3.2. Overdose/Toxicity

Digoxin intoxication usually occurs at doses that are higher than those needed to achieve a therapeutic effect (Smith and Haber, 1970). Digoxin increases $[Ca^{2+}]_i$. If $[Ca^{2+}]_i$ is excessively elevated, the situation is worsened by the fact that Ca^{2+} displaces Mg^{2+} from its binding sites because his will result in further elevation of the $[Ca^{2+}]_i$ by means of two mechanisms: (1) displaced Mg^{2+} causes the mitochondria to produce less ATP (Marx, 2005), which is necessary to either extrude excess $[Ca^{2+}]_{cyt}$ extracellularly or move it into the endoplasmic reticulum (ER) and (2) Na^+/K^+-ATPase uses ATP-Mg^{2+} as a substrate and if Mg^{2+} is displaced from the molecule then the enzyme will not have any substrate and therefore be effectively inhibited, which will be the beginning of a new cycle of elevation of $[Ca^{2+}]_i$ (Kurup and Kurup, 2002). Ca^{2+} homeostasis in the cell is discussed in more detail in a later section.

2.1.4. Use during pregnancy

The treatment for heart failure in pregnant woman largely follows conventional practice with loop diuretics, vasodilators with or without digoxin forming the cornerstone of initial intervention (James, 2004). Sustained tachyarrhythmias are the most important rhythm disturbances in the fetus, for which digoxin has been widely accepted as first line treatment (Krapp *et al.*, 2002). Because of its molecular structure, digoxin rapidly crosses the placenta and reaches

equilibrium, with maternal and foetal sera having equal concentrations (Soyka, 1975).

2.1.5. Neurological effects

Digoxin occurs naturally in the body. In the literature this molecule is called digoxin-like immunoreactive factor or ouabain-like compound. It is synthesized in the hypothalamus from its precursor, acetyl-coenzyme A and has the ability to modulate various neurotransmitter systems (Haupert, 1989; Ravikumar *et al.*, 2001). Hisaka *et al.* (1990) has shown that digoxin affects neutral amino acid transport through upregulating tryptophan transport over that of tyrosine. In tipping the scale of neutral amino acid transport it also affects the ratio of catabolites of tryptophan (serotonin, quinolinic acid, strychnine and nicotine) and tyrosine (dopamine, morphine and noradrenaline) in the brain, in this way modulating neurotransmitter systems. For example, low dopamine levels inhibit the mesolimbic-mesocortical dopaminergic system, which is associated with addiction and substance abuse and has been shown to correlate with elevated levels of endogenous digoxin (Kurup and Kurup, 2003). Dehydroepiandrosterone sulphate (DHEAS), a neurosteroid, interacts with γ-amino butyric acid (GABA) receptors in the brain. Uptake of DHEAS by cells from TM-BBB mice, is significantly inhibited by digoxin through its interaction with the oatp-2 transporter (Asaba *et al.*, 2000), in this way digoxin can promote excitotoxicity and adversely affect learning and memory ability in the brain. Digoxin could possibly affect the functionality and development of the nervous system during fetal exposure and research has associated digoxin with neurological disorders such as schizophrenia, epilepsy and autism (Kurup and Kurup, 2002).

2.2. BRAIN DEVELOPMENT

2.2.1. Neurulation

During the third week of gestation, following fertilization, the trilaminar germ disc forms through a process called gastrulation. This establishes the distinct layers in the disc: the ectodermal, mesodermal and endodermal germ layers. The central nervous system (CNS) derives from the ectodermal germ layer, from a structure named the neural plate. At the end of the third week of gestation, the lateral edges of the neural plate become elevated to form the neural folds with the neural groove in between. The two neural folds gradually approach each other until the meet and fuse around the area of the fifth somite, to form the neural tube. Fusion continues cephalocaudal until both the cephalic and caudal neuropores have closed, at day 27 of development (Sadler, 2000).

2.2.2. Brain vesicles

Following formation of the neural tube, three dilations develop in the cephalic region. These dilations are known as the primary brain vesicles, which are known as (from cephalic to caudal): the prosencephalon; the mesencephalon; and the rhombencephalon. These primary brain vesicles develop further until, at five weeks gestation, the prosencephalon consists of the telencephalon and diencephalon. By this time the rhombencephalon has also developed further to consist of the metencephalon and myelencephalon (Sadler, 2000). For a diagrammatic illustration of the development and adult derivatives see fig 2.2.

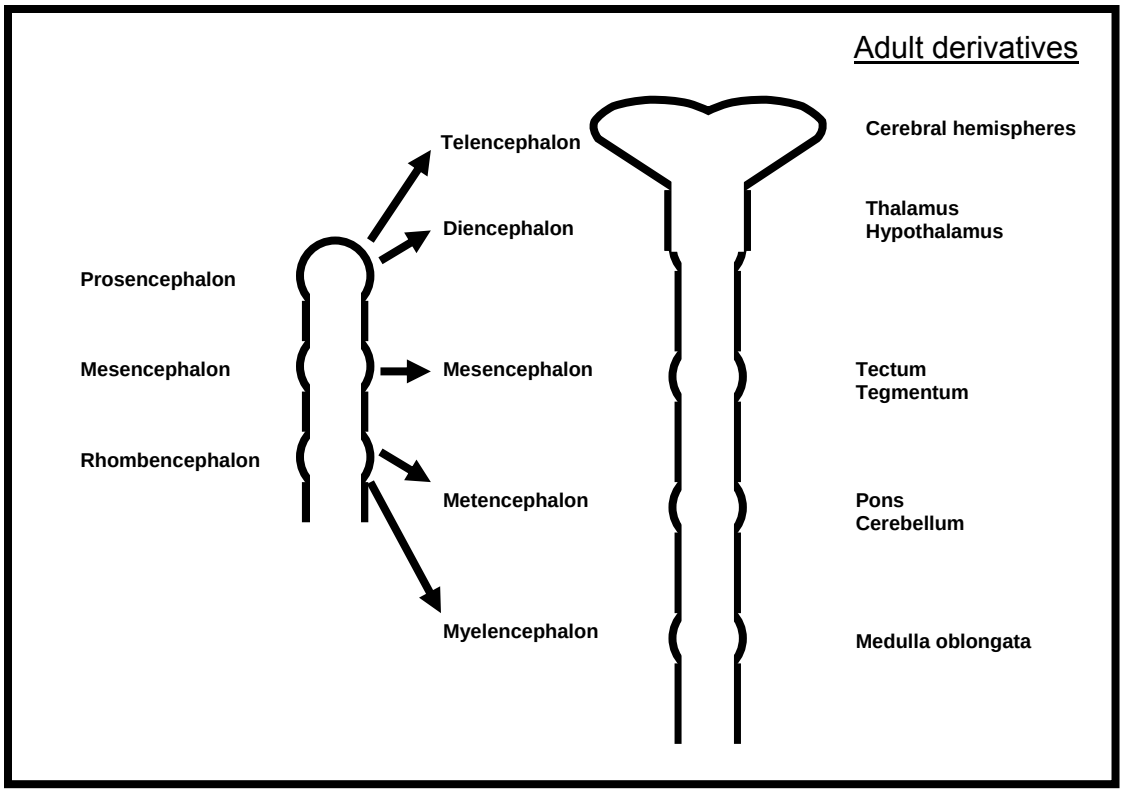

Fig. 2.2. Dorsal view of the neural tube illustrating the development of the brain vesicles and showing the adult derivatives.

2.2.3. Histological differentiation

Primitive nerve cells are known as neuroblasts. These cells originate exclusively from the neuroepithelial cells. Initially, neuroblasts are round, apolar cells but through further differentiation they develop two cytoplasmic elongations on opposite poles of the cell to form bipolar neuroblasts. One cytoplasmic process elongates rapidly to form the primitive axon and the other develops multiple smaller cytoplasmic processes to form primitive dendrites. These cells are known as multipolar neuroblasts, which, through further differentiation will become neurons.

The primitive supporting cells are known as gliablasts. These cells also originate from the neuroepithelial cells but only after the production of neuroblasts has

finished. Gliablasts differentiate into protoplasmic astrocytes, fibrillar astrocytes and oligodendroglial cells. Oligodendroglial cells are responsible for forming myelin sheaths around the axons of multipolar neuroblasts and neurons (Sadler, 2000).

2.2.4. Myelination

Myelininogenesis is the process by which specialized plasma membrane extensions ensheath neuronal axons (Campagnoni and Macklin, 1988) and is under tight regulation by developmental signals. Myelin is a tightly packed multilamellar membrane that wraps around axons to act as an electrical insulator and to increase conduction velocity. Approximately 50% of the total myelin protein in the CNS is composed of proteolipid protein, which is synthesized in the endoplasmic reticulum of oligodroglial cells (Bizzozero *et al.*, 2001). Myelination in the spinal cord starts at approximately four months of gestation. Most of the CNS remains unmyelinated until postnatal life. Motor fibres descending from the higher brain centres do not become myelinated until the first year of postnatal life and nervous system tracts only become myelinated once they start functioning (Sadler, 2000).

Digoxin may effect neuronal and brain development and to do so it would need to exert its effect on a cellular level by inhibiting Na^+/K^+-ATPase.

2.3. Na^+/K^+-ATPase

2.3.1. Structure

It is a heterodimeric enzyme consisting of two non-covalently linked subunits, designated α- and β-subunits. The 110kDa α-subunit protein molecule spans the membrane several times and contains the binding sites for ATP, cations and

specific inhibitors like the cardiac glycosides i.e. digoxin and ouabain (Sweadner,1989; Glynn, 1993). The α-subunit is further divided into four isoforms, designated α_{1-4}, which are present in different ratios throughout the different tissues of the body (Shull *et al.*, 1986; Herrera *et al.*, 1987; Orlowski and Lingrel, 1988). The α_1 subunit is present throughout the whole body and is the predominant species expressed in the kidneys, whereas the α_2 subunit is present in muscular as well as neuronal tissue. In the brain the α_1-subunit is expressed in both neurons and glia, the α_2-subunit is expressed predominantly in glia and the α_3-subunit exists exclusively in neurons (Mobasheri *et al.*, 2000; Sweadner 1989, 1992). Interestingly, Wang *et al.*, (2000) found that ouabain administered for six weeks increased the expression of α_1-subunit protein and mRNA in rat hypothalamus, but not that of $\alpha_{2,3}$.

The 55kDa β-subunit is a glycoprotein essentially necessary for assembly and transport of the α-subunit to the plasma membrane. Another function of the β-subunit is modulation of the α-subunit's affinity for Na^+ and K^+ (Geering *et al.*, 1996; Blanco and Mercer, 1998; Mobasheri *et al.*, 2000). It is also divided further into three isoforms, designated β_{1-3} (Shull *et al.*, 1986; Orlowski and Lingrel, 1988; Martin-Vasallo *et al.*, 1989).

2.3.2. Function

Na^+/K^+-ATPase falls in a group of P_2-type ATPases that use the hydrolysis of ATP to drive ion transport across cell membranes (Scarborough, 1999). Also known as the membrane sodium pump, it is necessary for the exchange of extracellular K^+ ($[K^+]_e$) for intracellular Na^+ ($[Na^+]_i$) in order to maintain the resting membrane potential across the plasma membrane of the cell. The pump exchanges two $[K^+]_e$ molecules for three $[Na^+]_i$ ions, ensuring a constant concentration gradient of these two ions across the plasma membrane. Not only are constant concentrations necessary for membrane potential but also for the

uptake of neurotransmitters and glucose, as well as the extrusion of Ca^{2+} from the cytoplasm (Sweadner, 1989).

According to Sokoloff (1993), Na^+/K^+-ATPase uses approximately 40%-50% of the ATP generated in the brain, which illustrates the importance of this enzyme in brain functioning. Literature has shown a close relationship between Na^+/K^+-ATPase and neurotransmission. This research suggested that the enzyme could play a role in the modulation of the neurotransmission mechanism. An example can be found in the cardiac glycoside, Ouabain, which selectively inhibits the functioning of Na^+/K^+-ATPase and increases neurotransmitter release, specifically acetylcholine, 5-hydroxytryptamine (serotonin) and catecholamines (Blasi *et al.*, 1998; Meyer and Cooper, 1981; Satoh and Nakazato, 1989; Stojanonic *et al.*, 1980).

By inhibiting Na^+/K^+-ATPase, digoxin in fact increases the concentration of Ca^{2+} within the cytosol, through reversing the action of the Na^+/Ca^{2+}-exchanger.

2.4. Ca^{2+}

2.4.1. Physiological maintenance of homeostasis

Under normal conditions the $[Ca^{2+}]_{cyt}$ concentration ranges between 10 and 100nM whereas $[Ca^{2+}]_e$ is between 1-2nM. This is almost a 100 000-fold Ca^{2+} gradient exist across the plasma membrane. Cellular Ca^{2+} homeostasis is maintained by energy-dependant pumps and directional transporters, the majority of which is located in the plasma membrane, endoplasmic reticulum (ER) and mitochondria (Berridge *et al.*, 2003; Carafoli *et al.*, 2001).

2.4.1.1. Ca^{2+} homeostasis and the plasma membrane

Ca^{2+} influx is controlled by ligand, voltage-gated and leak channels located in the plasma membrane. Influx is countered by the Na^{+}/Ca^{2+} exchanger and the plasma membrane Ca^{2+} ATPase (PMCA). Influx and efflux is finely controlled by these channels, pumps and exchangers to maintain the high concentration gradient across the plasma membrane (Dong *et al.*, 2006). See fig. 2.3.

2.4.1.2. Ca^{2+} homeostasis and the ER

One of the important roles of the ER in the cell is that of Ca^{2+} storage. Ca^{2+} concentrations within the ER can extend into the millimolars. The concentration gradient across the ER membrane is approximately 10 000-fold. Influx into the ER lumen is controlled by an energy dependant pump called the sarco-endoplasmic reticulum Ca^{2+}-ATPase or SERCA. Efflux from the ER is controlled by the inositol triphosphate receptor (IP_3R) upon stimulation by inositol triphosphate (IP_3) (Patterson *et al.*, 2004). In striated muscle, Ca^{2+} release is also controlled by the ryanodine receptor (RyR) upon Ca^{2+} binding. The latter process is called Ca^{2+}-induced Ca^{2+} release (Meissner, 2004). See fig. 2.3.

2.4.1.3. Ca^{2+} homeostasis and the mitochondrion

Normally Ca^{2+} concentrations in the mitochondrion is relatively low, approximately 100nM. However, apart from its other important functions, the mitochondrion also has a buffering function (Duchen, 2000). When $[Ca^{2+}]_{cyt}$ becomes to high, Ca^{2+} is rapidly absorbed by the mitochondrion and this buffering action allows it to regulate Ca^{2+} signals through localized interaction with the ER (Dong *et al.*, 2006). Ca^{2+} is absorbed into the mitochondrial matrix through a Ca^{2+} uniporter, which is activated once $[Ca^{2+}]_{cyt}$ reaches micromolar levels. Mitochondria also have a Na^{+}/Ca^{2+} exchanger, which extrudes Ca^{2+} from

the mitochondrial matrix. Under pathological conditions this exchanger can reverse its operation. See fig. 2.3.

2.4.2. Ca^{2+} and cell death

Apoptosis and necrosis are two forms of cell death. Necrosis is characterized by cellular swelling and organelle disruption, ending with loss of plasma membrane integrity. Apoptosis, on the other hand, is characterized by cellular shrinkage, membrane blebbing and condensation of organelles like the mitochondria and nucleus (Dong *et al.*, 2006). It has always been thought that these two mechanisms of cell death are mutually exclusive but recent evidence suggests that this might not be the case. Research shows that under specific circumstances these two mechanisms even occur simultaneously in liver and brain tissues, in a new process is called aponecrosis (Cheng *et al.*, 2003; Pretorius and Bornman, 2005).

Under pathological conditions where Ca^{2+} homeostasis is disrupted, the versatile nature of Ca^{2+} turns the ion into a powerful activator of multiple damaging processes. Toxicity can result from the direct effects of Ca^{2+}, indirectly through activation of degradative hydrolases, or from combinations of both processes.

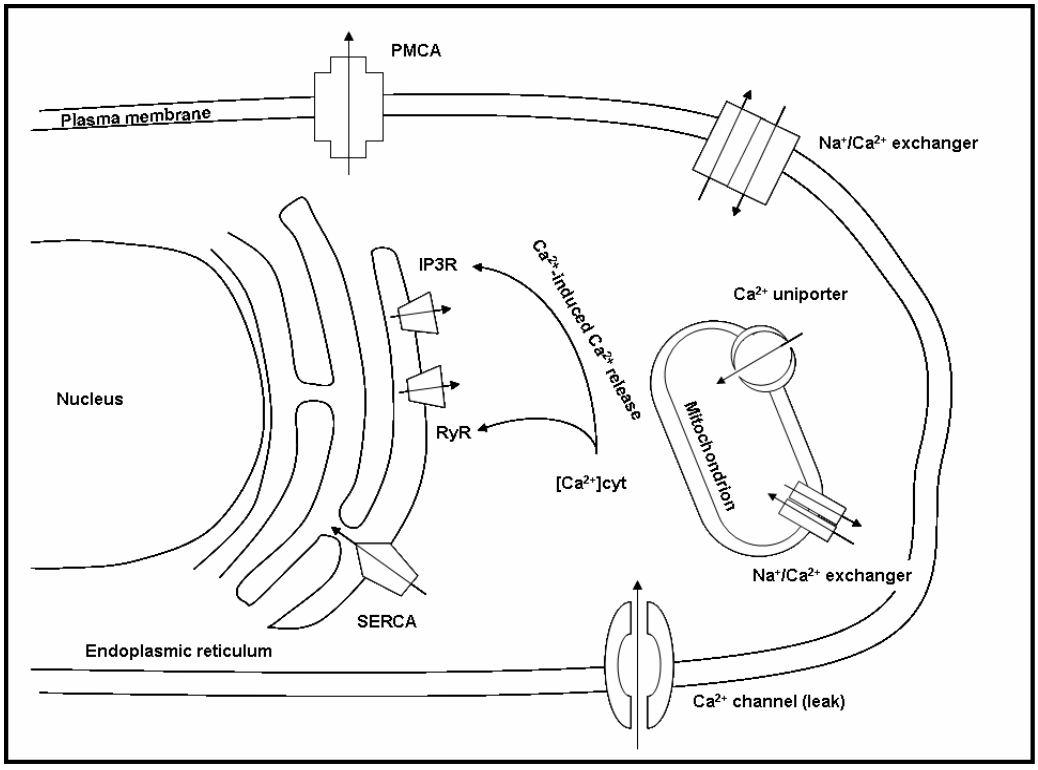

Fig. 2.3. A schematic illustration of cellular Ca^{2+} homeostasis.

PMCA = plasma membrane calcium ATPase; **IP3R** = inositol triphosphate receptor; **RyR** = ryanodine receptor; **SERCA** = sarco-endoplasmic reticulum calcium ATPase. Arrows indicate the direction into which Ca^{2+} is driven except at the Na^{+}/Ca^{2+} exchangers, located in the plasma and mitochondrial membranes, where Ca^{2+} is pumped into both the cytosol and mitochondrial matrix in exchange for Na^{+}.

2.4.2.1. Ca^{2+}-induced cell death through damage occurring in the cytosol

Examples of direct Ca^{2+} damage would be cellular and mitochondrial swelling as a result of osmotic pressure differences caused by the excess of ionised Ca^{2+} within the cytosol and Ca^{2+} densities or precipitates in the form of insoluble calcium phosphate and calcium hydroxyapatite that form in the mitochondrial matrix during cell death. Several isoforms of phospholipases can be directly activated by Ca^{2+} such as phospholipase A2. Phospholipases cleave phospholipids that play an important role in membrane integrity. Another family of hydrolyses that are indirectly activated by Ca^{2+} are the calpains. Calpains are cysteine proteases that cleave structural proteins such as spectrin, which will

induce disruption of the cytoskeleton and membrane blebbing (Vanderklish and Bahr, 2000; Liu *et al.*, 2004; Edelstein *et al.*, 1997).

2.4.2.2. Ca^{2+}-induced cell death through damage to the mitochondrion

Mitochondrial permeability transition or MPT results from the formation of pores in the mitochondrial membranes with a size exclusion limit of ≤1.5kDa, and has long been suspected to play a significant role in mitochondrial-mediated cell death (Dong *et al.*, 2006). MTP pores may form transiently during physiological functioning but become permanent following an injurious insult such as a Ca^{2+} overload in the cell (Crompton, 1999; Bernardi, 1999; Lemasters *et al.*, 1998). The intermembrane spaces of mitochondria contain many killer molecules, one of which is called cytochrome C which is known to induce apoptosis through caspase activation.

At the same time, MPT also results in the loss of mitochondrial homeostasis. Phospholipases that are also activated by Ca^{2+}, also damage the mitochondrial membranes. MPT and activated phospholipases can cause the loss of mitochondrial membrane potential, which results in the cessation of the cells energy production and complete loss of cellular homeostasis. Cells depleted of energy die by means of necrosis (Crompton, 1999; Bernardi, 1999; Lemasters *et al.*, 1998).

From this it can be seen that mitochondrial damage plays a critical role in both the apoptotic and necrotic mechanisms of cell death.

2.5. SEROTONIN

Serotonin or 5-hydroxytryptamine is synthesised from the amino acid tryptophan by the enzyme tryptophan hydoxylase (Kuhn *et al.*, 1978; Hamon *et al.*, 1978). Serotonin is a monoamine neurotransmitter and has been shown to play a role in brain development prior to assuming its role a neurotransmitter (Chubakov *et al.*, 1986; 1993). Serotonin, as a neurotransmitter, modulates mood, emotion, sleep and appetite and has been implicated in numerous behavioural disorders such as depression (Schloss and Williams, 1998). Endogenous digoxin in the body has been suggested to cause a tip in the balance of amino acids entering the brain, specifically increasing tryptophan uptake into the brain, which results in increased serotonin levels in the brain (Hoshino, 1986).

2.6. SUMMARY

Literature suggests that for the treatment of chronic heart failure in pregnant woman and tachyarrhythmias in the fetus, digoxin is the drug of choice (James, 2004; Krapp, 2002). Digoxin inhibits Na^+/K^+-ATPase disturbing the resting membrane potential of cells, which plays a very important role in conductive tissues such as the brain, where neurons utilize the membrane potential to convey information in the form of action potentials. Also, the drug induces elevated levels of $[Ca^{2+}]_i$, which can influence intra- as well as intercellular signaling and possibly cell death through apoptosis, necrosis or a combination of both mechanisms.

Chapter 3:

The effect of digoxin on ultra-structural morphology *in ovo*, using the chick embryo model.

3.1. INTRODUCTION

Prenatal human development is divided into the embryonic period and the foetal period of development. The embryonic period occupies the first 8 weeks of development from fertilization and during this period the embryo develops from a one-celled creature into an organism which would be anatomically recognized as a human foetus. From 8 weeks on, during the foetal period, the foetus simply increases in size until birth (Sadler, 2000).

The embryonic period is divided into 23 embryonic or Carnegie stages according to age, size and morphological features (O'Rahilly and Müller, 1987; 1999). The importance of Carnegie stages is that it allows for the comparison of embryonic development between different types of organisms because it eliminates chronological age and size and focuses on pivotal developmental features of the embryo's morphology. For example, one can compare a chicken embryo model's development to human embryo development as long as both embryos are in the same Carnegie stage of development because all embryos develop more or less the same in the early stages.

All the major subdivisions of the brain are established between Carnegie stages 12 - 23 or developmental days 26 - 56 (O'Rhailly and Müller, 1987; 1999). Myelination within the CNS is hierarchical. At birth only the structures necessary for survival are myelinated, in particular the spinal cord, brain stem and

cerebellar peduncles. After birth, myelination in humans may continue into the third decade of life and the structures in which myelination occur this late after birth are necessary for higher brain functions such as reasoning (Reißenweber *et al.*, 2005).

3.2. MATERIALS

3.2.1. Chick embryos

Fertile Broiler Hatching eggs were obtained from National Chicks hatchery in Pretoria, South Africa.

3.2.2. Reagents

Ethanol, formaldehyde, gluteraldehyde $NaH_2PO_4.H_2O$ and Na_2HPO_4 were purchased from Merck in Johannesburg, South Africa. OsO_4 was purchased from Spi-Chem suppliers, West Chester PA, 19381, USA.

Digoxin was purchased in powder form from Sigma-Aldrich, Aston Manor, South Africa.

3.3. METHOD

3.3.1. Inoculation technique

Fertile Broiler Hatching eggs were incubated in a Grumbach incubator at 37°C in humidified air and inoculated at Carnegie stages 4 and 6. The digoxin solution was administered onto the chorionic-allantoid membrane (CAM) via pre-drilled holes on the blunt end of each egg. Following the first inoculation (at Carnegie

stage E4), the pre-drilled holes were closed by using candle wax to assure that the connection with the external environment was completely sealed off. New holes were drilled for the second inoculation at Carnegie stage 6 and again sealed off with candle wax. Embryos were terminated at Carnegie stage 8 and brains carefully dissected and immediately fixed in 2,5% gluteraldehyde prepared in distilled water to avoid the morphological manifestation of any post-mortem damage in the neural tissue.

All manipulations were done under sterile conditions in a laminar flow hood and all laboratory work was done in accordance with the ethical committee of the University of Pretoria.

3.3.2. Dosages

The digoxin powder was made up to a 6.4µM solution containing 50% EtOH. This concentration is the same as that of commercially available forms of digoxin such as Lanoxin®. Eggs were divided into six groups with five eggs in each group. One egg in each group was used as a control and was administered an equal amount of a 50% ethanol solution containing no drug. The following concentration range was used:

Table 3.1. Schematic illustration of the method used to determine an effective concentration range.

	Controls	Dosage			
Group 1	2,5µL 50% EtOH	16nM digoxin 50% EtOH	16nM digoxin 50% EtOH	16nM digoxin 50% EtOH	16nM digoxin 50% EtOH
Group 2	5µL 50% EtOH	32nM digoxin 50% EtOH	32nM digoxin 50% EtOH	32nM digoxin 50% EtOH	32nM digoxin 50% EtOH
Group 3	10µL 50% EtOH	64nM digoxin 50% EtOH	64nM digoxin 50% EtOH	64nM digoxin 50% EtOH	64nM digoxin 50% EtOH
Group 4	15µL 50% EtOH	96nM digoxin 50% EtOH	96nM digoxin 50% EtOH	96nM digoxin 50% EtOH	96nM digoxin 50% EtOH
Group 5	20µL 50% EtOH	128nM digoxin 50% EtOH	128nM digoxin 50% EtOH	128nM digoxin 50% EtOH	128nM digoxin 50% EtOH
Group 6	40µL 50% EtOH	256nM digoxin 50% EtOH	256nM digoxin 50% EtOH	256nM digoxin 50% EtOH	256nM digoxin 50% EtOH

3.3.3. Preparation of the neural tissue for scanning (SEM) and transmission electron microscopy (TEM)

After termination of the embryos, brains were carefully dissected and immediately fixed in a mixture of 2,5 % gluteraldehyde and 2,5% formaldehyde in 0,075M $NaPO_4$ phosphate buffer with a pH of 7,4. Following the initial fixation, which lasted between 2-4 hours, the neural tissue was rinsed three times (10-15 min per wash) in phosphate buffer. Rinsed material was then post-fixed in a 1% aqueous OsO_4 solution for a period of 1-2 hours. Material was rinsed another

three times in phosphate (10-15 min per wash). After fixation, the material was serially dehydrated in 30%, 50%, 70%, 90% and three times in 100% EtOH.

For evaluation with the TEM, dehydrated material was embedded in Epoxy Resin (Van der Merwe and Coetzee, 1992), followed by ultra-microtome sectioning and then stained with a 4% aqueous uranyl acetate solution and lead citrate. Examination of the sections was performed using a Phillips TEM.

For evaluation with the SEM, dehydrated material was dried in a critical point drier, after which it was coated with a conductive RuO_4 coating. Coated specimens were mounted and examined using a JEOL 6000F FEGSEM, Field Emission Microscope.

3.4. RESULTS AND DISCUSSION

3.4.1. Control group (Exposed to EtOH alone)

Even at low concentrations the ethanol solution caused noticeable damage to the neurons from the control brains. Damage manifested in both the plasma and nuclear membranes (fig. 3.1a and 3.1b). Fig. 3.1a shows rupture of both the nuclear and plasma membranes. Figure 3.1b shows damage to the plasma membrane in the form of a rough appearance of the cell surface rather than a smooth and wavy appearance. Fig. 3.2a shows significant cellular swelling. In addition to the damage mentioned fig. 3.2b demonstrates a dilated endoplasmic reticulum and a slightly swollen mitochondrion. The aforementioned are all characteristics indicative of cellular death by necrosis.

It should be noted that control groups exposed to 40µL EtOH did not develop and the micrographs presented here represent the worst damage that occurred in the control brains exposed to low concentrations of EtOH. Therefore, these

micrographs show the largest impact that the utilized ethanol concentration alone may have on neuronal ultrastructure. For example, fig. 3.1a shows considerable damage to the nuclear and plasma membranes, whereas in fig. 3.2a nuclear and plasma membranes seem intact.

EtOH is capable of inducing both apoptosis and necrosis in human and rat hepatocytes depending on the concentration of ethanol that the cells are exposed to (Castilla *et al.*, 2004). The occurrence of apoptosis increases with EtOH concentration. In contrast, necrosis is inhibited at intermediate concentrations (1-2mmol/L in humans) and sharply increases at high concentrations (10mmol/L) (Castilla *et al.*, 2004). In the brain, EtOH-induced cell death can be caused in several different ways: (1) increasing free radicals such as reactive oxygen species (ROS); (2) decreasing anti-oxidant capacity within the cell caused by a toxic insult (ethanol); and (3) damaging mitochondria causing mitochondrial permeability transition (MPT). The latter releases caspases, cytochrome C and Ca^{2+} into the cytoplasm, ultimately resulting in cell death (Goodlett and Horn, 2001). This effect can be seen in fig. 3.2b, which shows minor reversible damage to the mitochondrium (arrow).

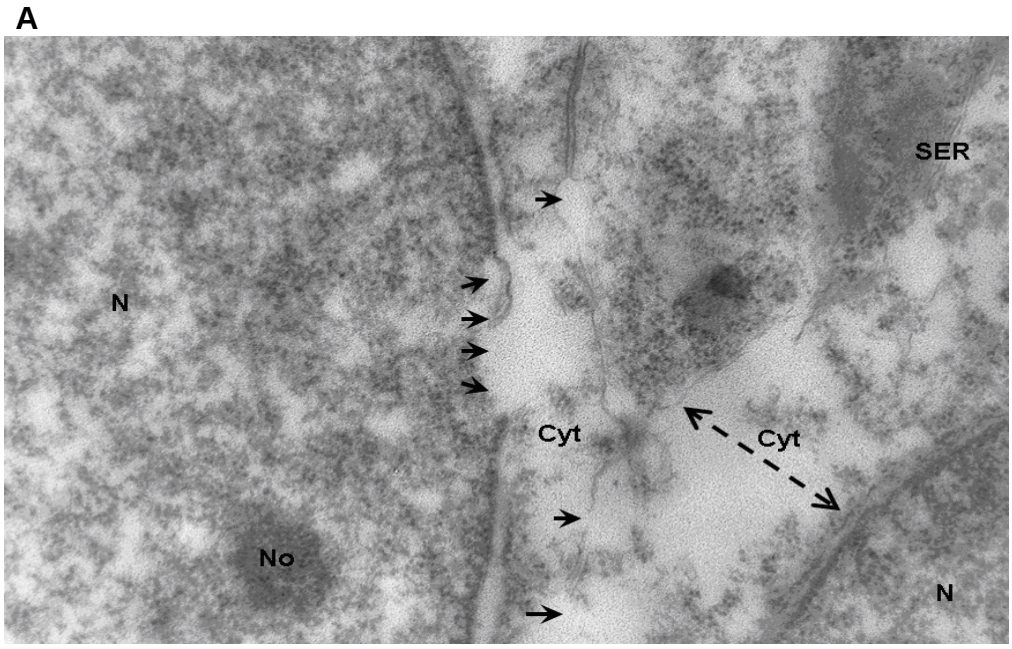

Fig. 3.1A. TEM micrograph of control chick embryo brain exposed to 5µL 50% EtOH. ***N*** = nucleus; ***No*** = nucleolus; ***Mt*** = mitochondrium; ***SER*** = smooth endoplasmic reticulum; ***Cyt*** = cytoplasm. Notice the damage to both the nuclear and plasma membranes (arrows) as well as swelling of the cytoplasm (dashed line), indicative of necrosis. 28 000 × magnification.

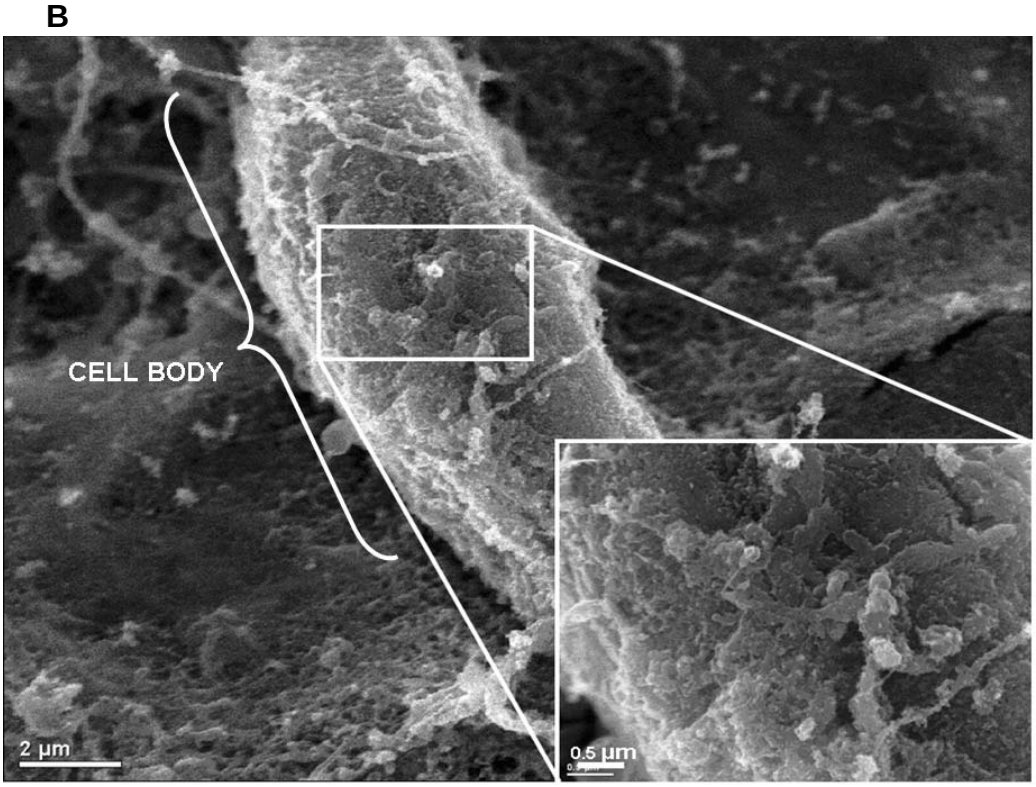

Fig. 3.1B. SEM micrograph of control chick embryo brain exposed to 10µL 50% EtOH. Significant damage to the plasma membrane can be seen as the rough appearance of the cell surface. Scale bar of inset = 0.5µm.

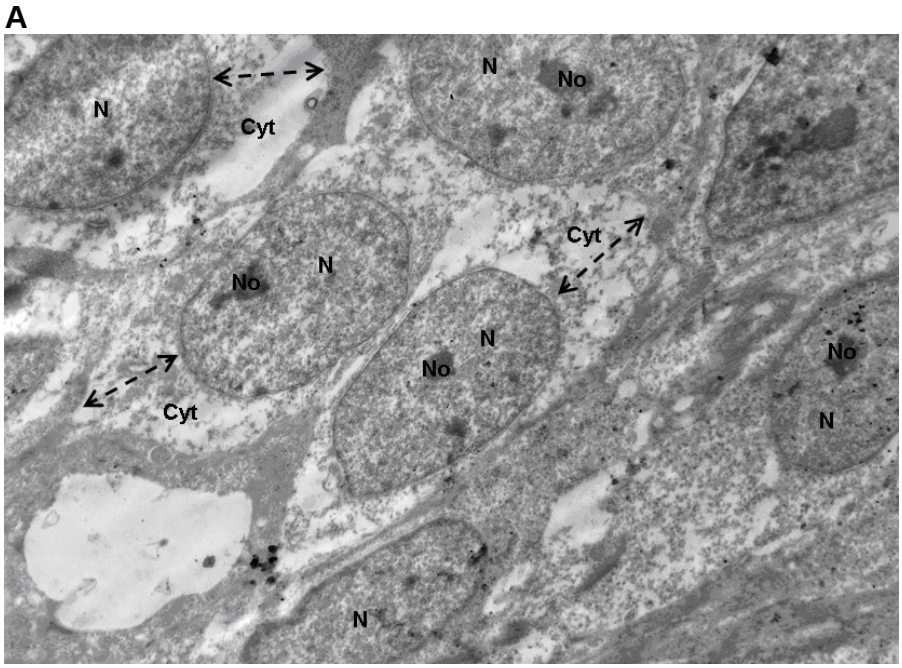

Fig. 3.2A. TEM micrograph of control chick embryo brain exposed to 5µL 50% EtOH. ***N*** = nucleus; ***No*** = nucleolus; ***Cyt*** = cytoplasm showing swelling. Notice the amount of swelling of the neuronal cytosols (dashed lines), indicative of necrosis. 4 300 × magnification.

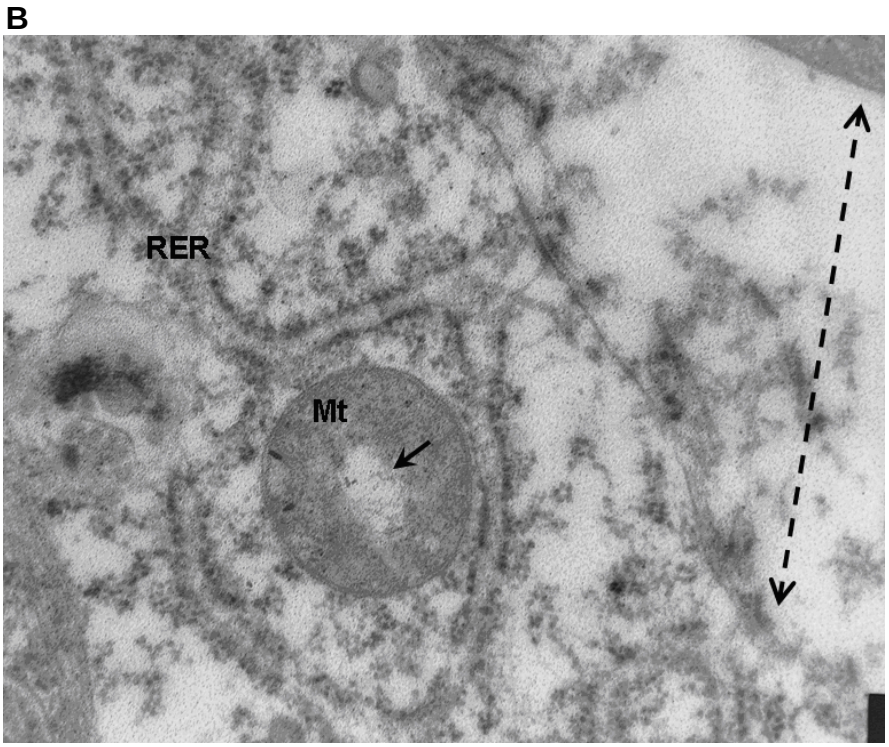

Fig. 3.2B. TEM micrograph of experimental chick embryo brain exposed to 5µL 50% EtOH. ***RER*** = rough endoplasmic reticulum; ***Mt*** = mitochondrium. Reversible mitochondrial damage (arrow). Cellular swelling is visible in the dispersion of cytoplasmic contents (dashed line). 36 000 × magnification.

3.4.2. Experimental digoxin group (low dose)

At low concentrations of digoxin exposure (32nM in 50% EtOH), damage to the plasma membrane of neurons is prominent in comparison to that of control brains (EtOH alone). This is best illustrated in fig. 3.3a, which shows the granular, almost unrecognisable appearance of the plasma membrane as compared to a neuron that has not been exposed to any substance (fig. 3.3b). The reason necrosis appears more prominent in these neurons is most probably because digoxin increases $[Ca^{2+}]_i$. In *section 3.4.1.* it was stated that ethanol, through mitochondrial damage, can also increase $[Ca^{2+}]_i$. Increased Ca^{2+} in the cytosol will also contribute to the damaging effect on mitochondria, enhancing the MPT, which releases more Ca^{2+}. Increased cytosolic Ca^{2+} also induces Ca^{2+}-induced Ca^{2+} release from the endoplasmic reticulum, which enhances the effects of the elevation of $[Ca^{2+}]_i$ (Meissner, 2004). This will result in a dramatic increase in $[Ca^{2+}]_i$ when compared to ethanol exposure alone. This increase in $[Ca^{2+}]_i$ slowly increases the osmotic pressure within the cell, and result in slow, but significant cellular swelling, which will compromise plasma membrane integrity and therefore cause necrosis, as seen in fig. 3.3a.

Damage to the nuclear membrane is indicated by the arrows in fig. 3.4. In this case damage occurred not in the form of membrane rupture, as is the case in control brains (exposed to EtOH alone), but presented as detachment of the inner- from the outer nuclear membrane. The damage observed here is not typical of necrosis but rather of apoptosis. To the left of the nucleolus are three dense chromatin bodies which could represent one of two phenomena: 1) multiple nucleoli or 2) condensation of the chromatin in a number of different nuclear bodies typical in apoptosis. The membrane damage could also be interpreted as the beginning of nuclear fragmentation, indicating apoptosis.

Dilation of the endoplasmic reticulum (fig. 3.4) is possible during apoptosis but is more likely during necrosis. Other characteristics that support necrosis are swelling of the cytoplasm and the fact that slight mitochondrial swelling is present. Severe mitochondrial damage can be seen in fig. 3.5. The arrows indicate areas of mitochondrion distension and complete disruption of the normal internal morphology of the mitochondrion. Matrix densities are also visible. This degree of mitochondrial damage rules out the possibility of cell death by apoptosis because apoptosis requires energy, which cannot be provided by the mitochondria if they are damaged.

A possible explanation for the contradicting characteristics is that both apoptosis and necrosis are occurring simultaneously. Previous research has described a process that presents characteristics of both apoptosis and necrosis named aponecrosis (Cheng *et al.*, 2003; Pretorius and Bornman, 2005).

During the initial stages of damage, both apoptosis and necrosis probably occurred simultaneously, but ultimate cell death would most probably occur through necrosis because of the extent of mitochondrial damage, which would severely compromise cellular energy metabolism causing a significant drop in adenosine triphosphate (ATP). This will result in of cell death by apoptosis.

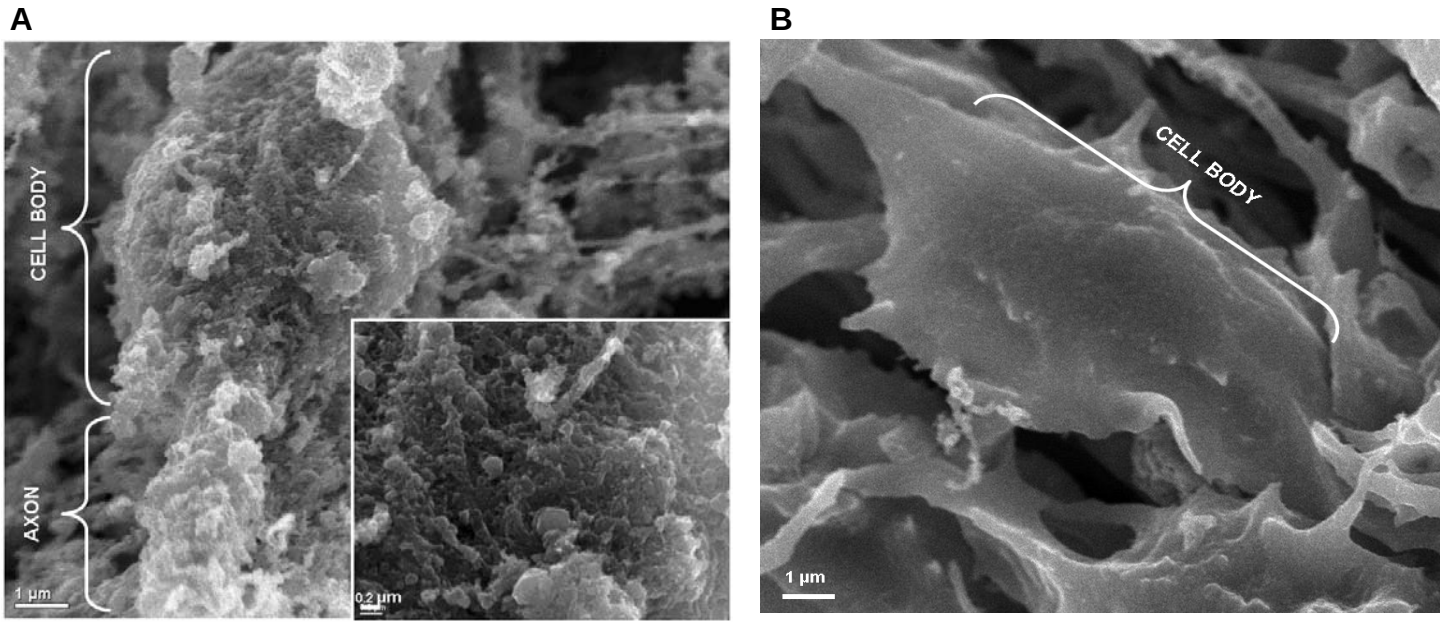

Fig. 3.3. (A) SEM micrograph of experimental chick embryo brain exposed to 32nM digoxin in 50% EtOH. The neuron has suffered significant membrane damage when examining the surface of the cell body, better seen in the inset. Scale bar of inset = 0.2µm. **(B)** SEM micrograph of chick embryo brain not exposed to digoxin or ethanol (Marx, 2005). Notice the smooth appearance of the surface of the cell body.

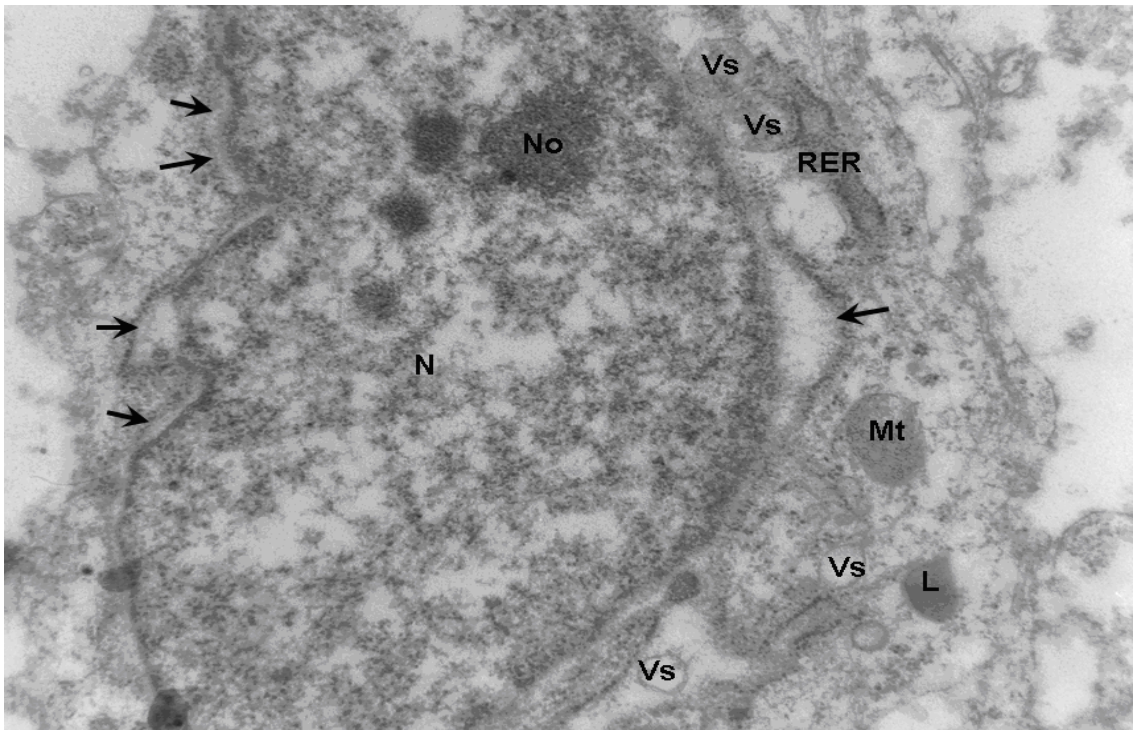

Fig. 3.4. TEM micrograph of experimental chick embryo brain exposed to 16nM digoxin in 50% EtOH. ***N*** = nucleus; ***No*** = nucleolus; ***Mt*** = mitochondrium; ***RER*** = rough endoplasmic reticulum; ***Vs*** = vesicle; ***L*** = lysosome-like dense body. The inner and outer membranes of the nuclear envelope have separated (arrows). 22 000 × magnification.

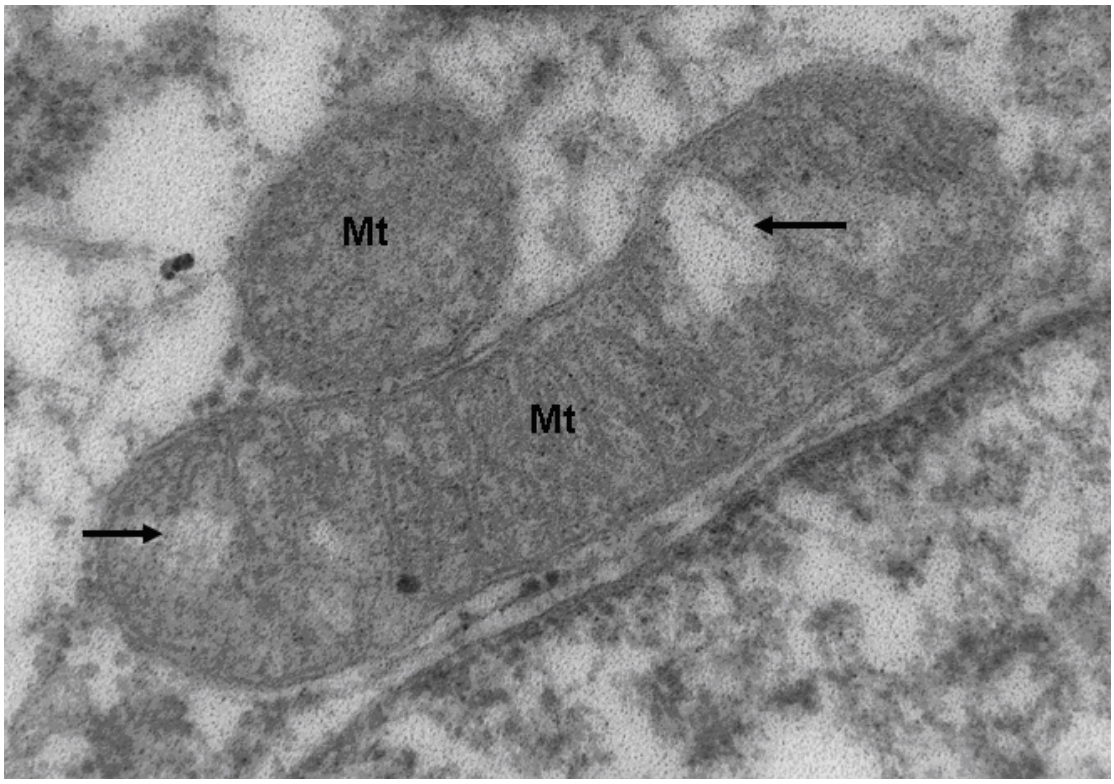

Fig. 3.5. TEM micrograph of experimental chick embryo brain exposed to 16nM digoxin in 50% EtOH. ***Mt*** = mitochondrium. Clearly visible is disruption of the nuclear envelope (circled). Considerable damage has occurred to the mitochondrium that may still be reversible (arrows). 43 000 × magnification.

3.4.3. Experimental group (high dose)

Group 6 in table 3.1 were exposed to 256nM digoxin in 50% EtOH. Exposure at this dosage was lethal in both the control and experimental groups as none of the embryos in group 6 developed.

Dosages of 128nM digoxin in 50% EtOH (group 5, table 3.1) yielded some startling results. Figure 3.6, especially 3.6a, shows advanced myelination of neurons within the CNS. With the inoculation technique used (*section 3.3.1.*), embryo's were terminated at Carnegie stage 8, which means that the embryo's still have to undergo development through stages 9 - 23, before they enter the foetal period. In the introduction to this chapter, it was stated that all the major subdivisions of the brain are established during Carnegie stages 12 - 23 (O'Rahilly and Müller, 1987; 1999) and that only the CNS structures necessary for survival are myelinated at birth. This is abnormal when compared to both the control and low dose arms of the experiment.

Fig. 3.6a shows highly magnified myelination around three axons. Myelination is visible as the concentric dark lamellae surrounding a white area in the centre. These lamellae are cytoplasmic processes of oligodendrocytes which are wrapped around the axonal process several times, ensheathing it and forming a myelinated fibre. Fig. 3.6b shows an electron micrograph taken at low magnification. This micrograph serves the purpose of demonstrating the extent of myelination that has occurred within these brains, indicated by the arrows. Fig. 3.9a is a micrograph taken on a SEM, showing an axon protruding from the perikaryon of the neuron. What is remarkable about this very fortunate micrograph is the fact that it shows the myelin sheath, indicated by the arrows, surrounding the axon. Fig. 3.9b shows this same axon at a higher magnification, showing more detail. The inset in fig. 3.9b shows the entire length of the axon up to where it was severed during the preparation for SEM.

Fig. 3.6b and fig. 3.7 show the degree of differentiation that has already taken place within these brains. Glial cell processes can be seen extending throughout the brain, acting as supporting architecture for neurons in the CNS as they are organized into the three-dimensional structure or macroscopic anatomy of the brain. Fig. 3.8 is a particularly interesting micrograph captured at this embryonic age, when considering organizational differentiation of the brain. This micrograph shows a myelinated nerve bundle. This is most probably a nerve tract in the brain, seeing that it is developing this early. Glial cell processes are also demonstrated in fig. 3.10. Fig. 3.10a is a low magnification micrograph to show the amount of glial cell processes present in these brains and fig. 3.10b shows one of these processes at high magnification also showing the plasma membrane of an adjacent cell, supported by this process.

As was seen in the low dose experiments, signs of necrotic cell death are also present in the high dose experiments. In fig. 3.11 the extent of plasma membrane damage is visible. Also, severe mitochondrial damage has occurred as indicated in fig. 3.6a and fig. 3.10b. For more detail on the cell death caused by digoxin refer to the discussion on the low dose experimental results in *section 3.4.2.*

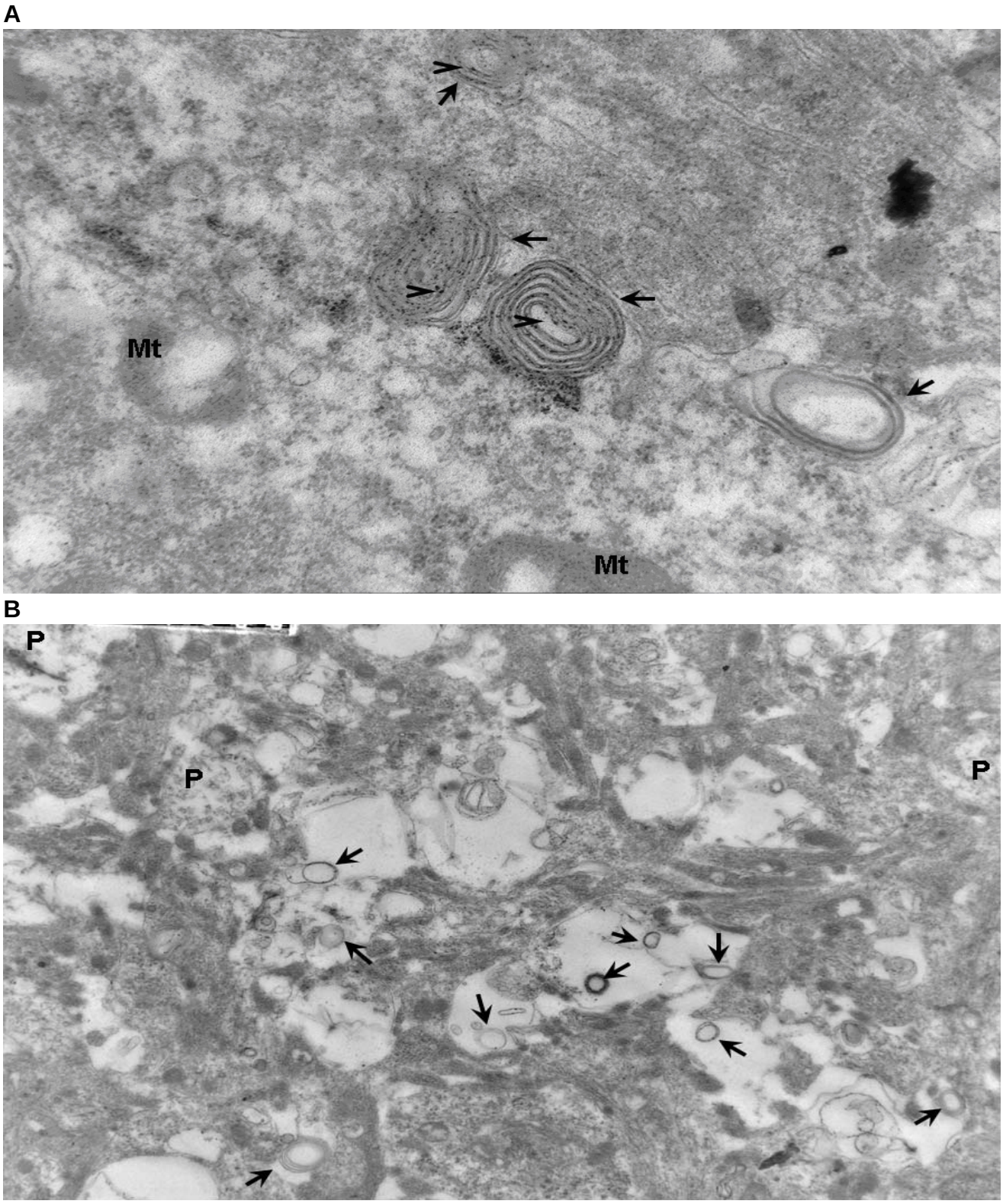

Fig. 3.6. TEM micrographs of experimental chick embryo brain exposed to 128nM digoxin in 50% EtOH. ***N*** = nucleus; ***Mt*** = mitochondrium; ***P*** = Glial cell processes acting as support and packing for neural structures; ***T*** = microtubules. Myelination of neurons can be seen as concentric dark circles (arrows) with a number of ribosomes present in each dark line (arrowheads). Non-reversible damage to some mitochondria is visible. **(A)** 75 000 × magnification; **(B)** 7 500 × magnification.

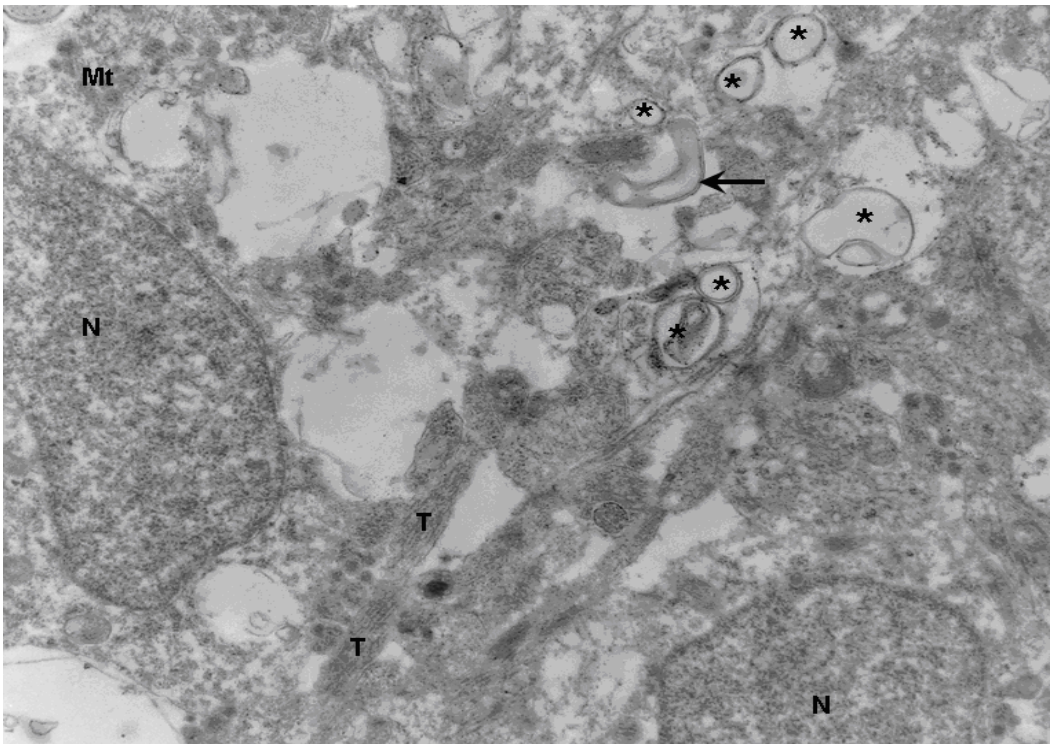

Fig. 3.7. TEM micrograph of experimental chick embryo brain exposed to 128nM digoxin in 50% EtOH. ***N*** = nucleus; ***Mt*** = mitochondrium; ***T*** = microtubules; ***Asterisk*** = myelinating axons. Longitudinal section of a myelinating axon (arrow). 9 800 × magnification.

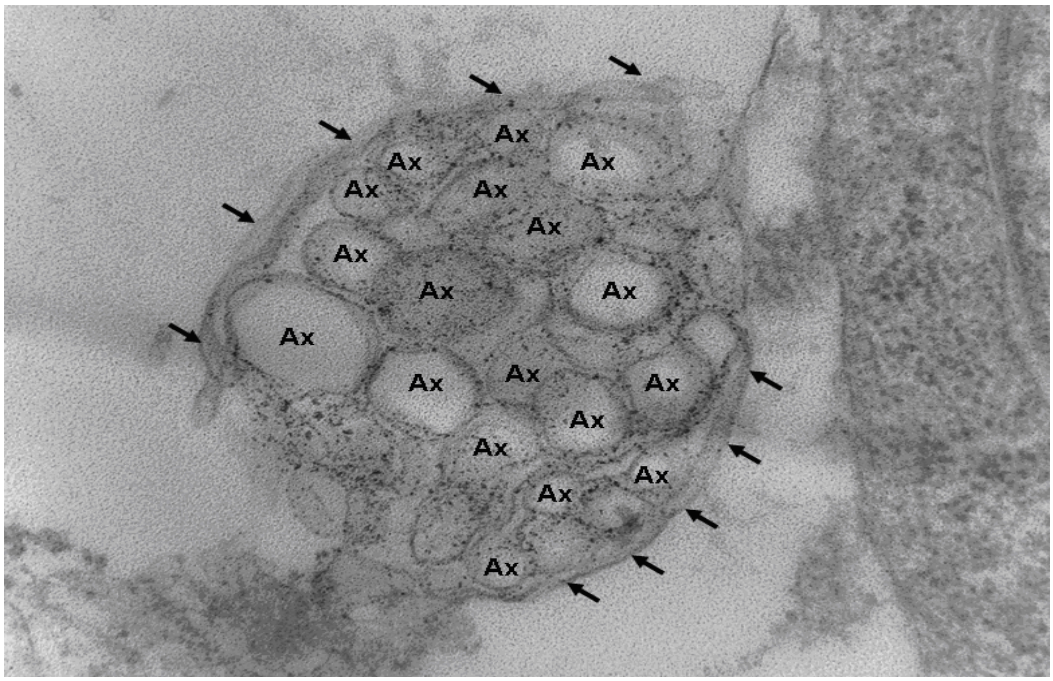

Fig. 3.8. TEM micrograph of experimental chick embryo brain exposed to 128nM digoxin in 50% EtOH. ***Ax*** = axon. Nerve bundle being encapsulated through myelination (arrows). 43 000 × magnification.

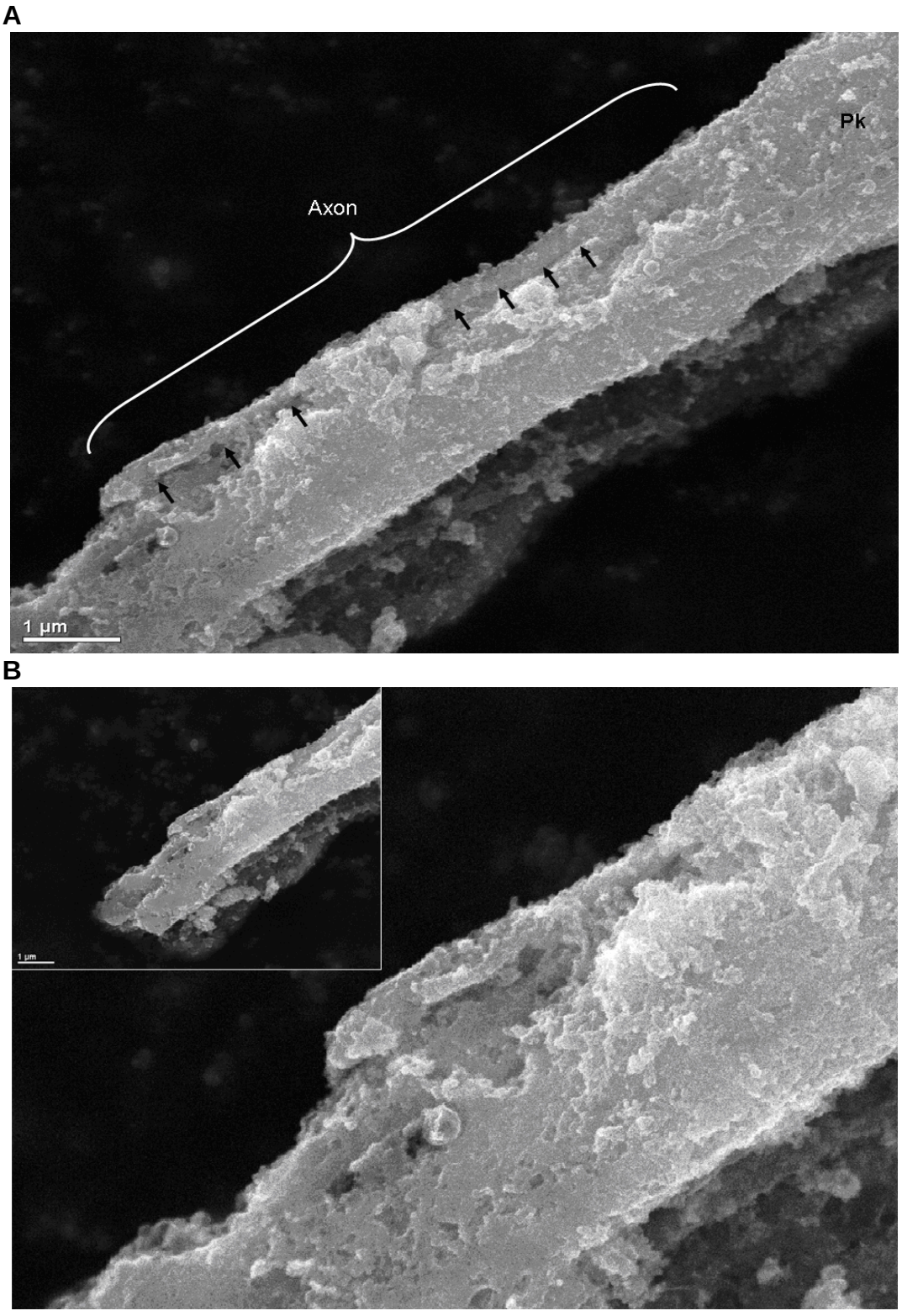

Fig. 3.9. Myelinated axon of neuron exposed to 128nM digoxin in 50% EtOH. ***Pk*** = perikaryon. **(A)** This SEM micrograph shows the axon extending from the distal neuronal cell body. The arrows indicate the plane between the myelin layer surrounding the exposed axon. **(B)** More distal shot of the axon in **(A)** and a higher magnification micrograph. Myelin-covered and exposed areas of the axon are clearly visible in the inset in **(B)**.

A

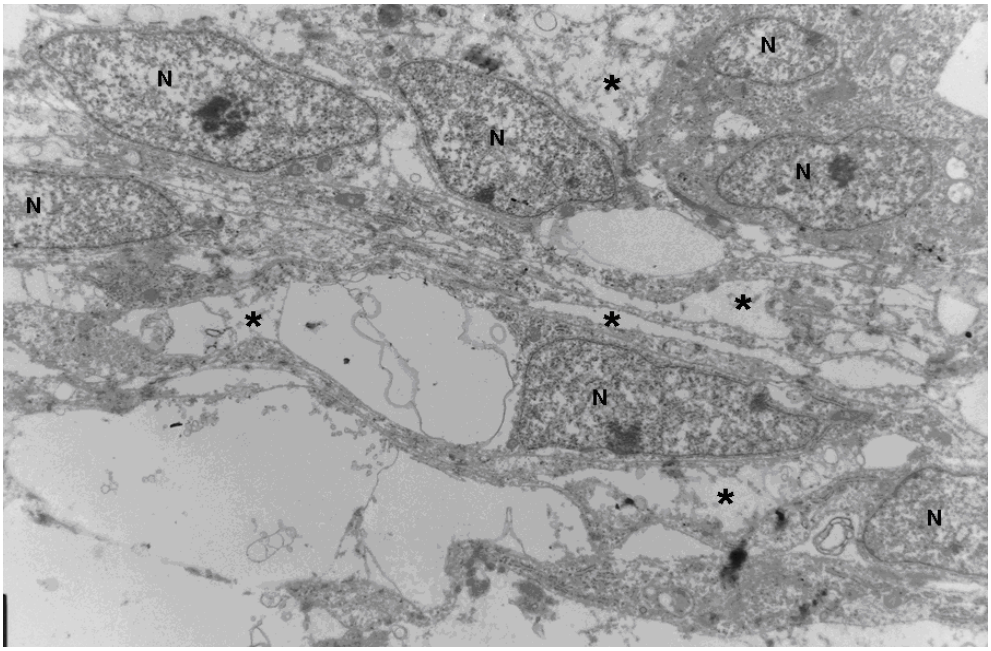

Fig. 3.10A. TEM micrograph of experimental chick embryo brain exposed to 128nM digoxin in 50% EtOH. ***N*** = nucleus; ***Asterisk*** = Glial cell processes acting as support and packing for neural structures. Morphologically brain structure and organization is much more advanced as compared to control brains. 4 300 × magnification.

B

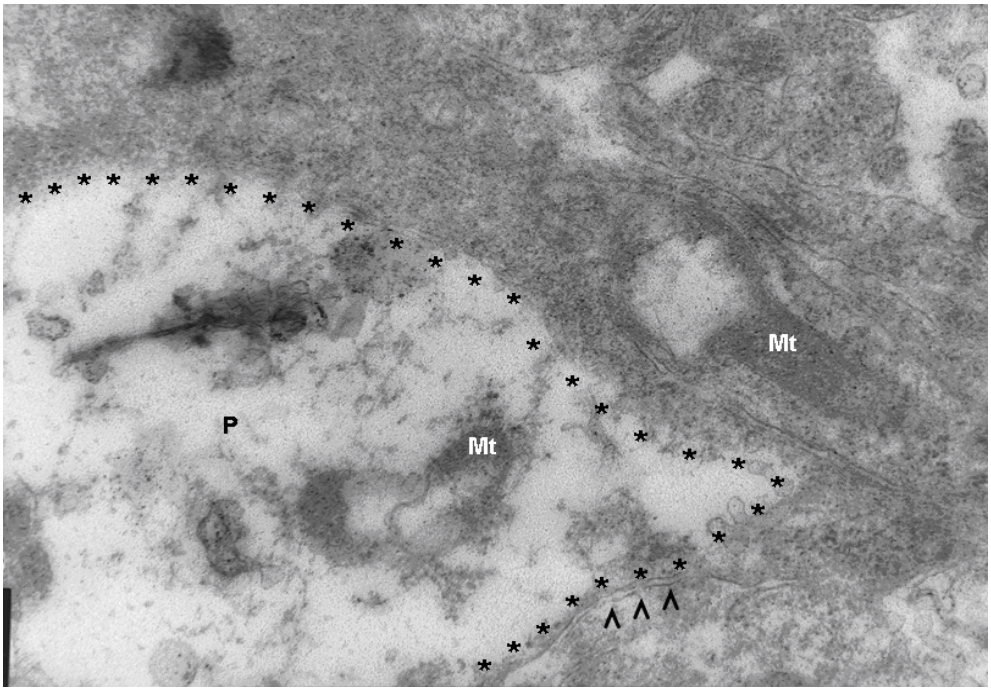

Fig. 3.10B. TEM micrograph of experimental chick embryo brain exposed to 128nM digoxin in 50% EtOH. ***Mt*** = mitochondrium; ***P*** = glial cell process; ***Asterisk*** = outline of a glial cell process. High magnification of a glial cell process. A juxtapositioned cell's plasma membrane is indicated by the arrowheads. Severely damaged mitochondria. 28 000 × magnification.

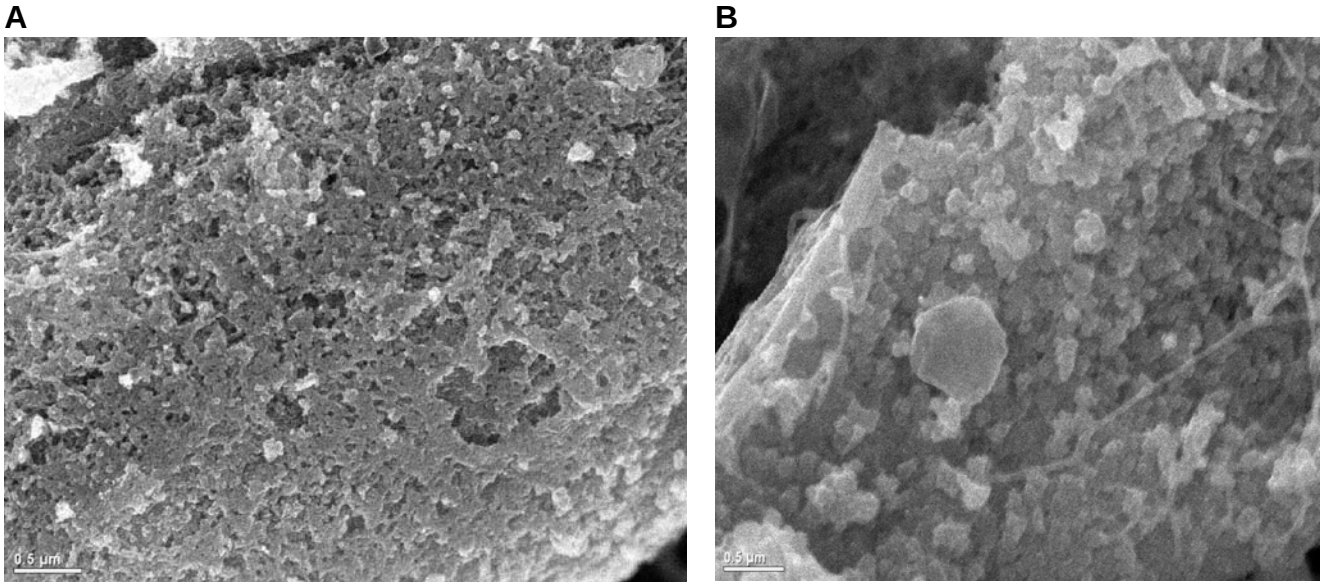

Fig. 3.11. (A) SEM micrograph of the surface of a neuron cell body from brain exposed to 128nM digoxin in 50% EtOH. **(B)** SEM micrograph of the surface of a neuron cell body from brain exposed to 20µL 50% EtOH. Scale bars in both micrographs = 0.5µm.

3.5. CONCLUSIONS

Conclusions that can be drawn from this chapter are:

1. Ethanol initiate (but don't necessarily result in) cell death in neurons *in ovo* at concentrations of 32nM (50% EtOH) and higher, predominantly by means of necrosis. Mitochondrial damage caused may still be reversible but membranous damage could be fatal.

2. Digoxin at concentrations of 16nM and higher (in 50% EtOH) *in ovo*, significantly increases the damage caused to neurons by EtOH alone. The mitochondrial damage observed would probably result in an increase in $[Ca^{2+}]_i$ and consequently cell death. Cells exposed to digoxin show a greater degree of cellular damage than cells exposed to ethanol alone (where appropriate controls have been included).

3. Severe mitochondrial damage of neurons following exposure to ethanol and digoxin indicates that cell death occurs by necrosis rather than apoptosis.

4. Digoxin at concentrations of 128nM (in 50% EtOH) *in ovo*, induces premature myelinogenesis and rapid structural organization of brain matter in the embryo. A possible theory to this will be discussed in the Concluding Discussion chapter (*Chapter 6*).

5. In order for myelinogenesis to occur, there must be differentiation of oligodendrocytes (Roots, 1995) and associated protein synthesis, specifically myelin basic protein. Thus, digoxin induces oligodendrocyte differentiation and protein synthesis associated with myelinogenesis.

3.6. FUTURE RESEARCH

The high dose experiment could be repeated but the embryos could perhaps be terminated at different Carnegie stages, which will show when myelinogenesis is initiated.

Dimethyl sulphoxide (DMSO) could be used as solvent for digoxin (Kang and Weiss, 2002) instead of EtOH (although it is known that DMSO is also cytotoxic at high doses). This would allow the assessment of the influential role that EtOH played in the current experiment. It would eliminate EtOH from having any effect on the premature myelinogenesis and rapid structural organization of the brain as seen in the high dose section of the experiment. By repeating the low dose experiment, it would give the investigator a better idea of whether digoxin would induce cell death because DMSO would, unlike EtOH, probably not increase $[Ca^{2+}]_i$ and therefore not enhance this effect of digoxin. It would also shed light on whether digoxin induces cell death through necrosis or apoptosis.

After brains are dissected from the embryos, it could be examined using light microscopy by making sections of the brains and staining specifically for myelin such as Salthouse's Luxol-fast blue G method (Salthouse, 1964). This would confirm the results obtained in this experiment and provide an idea of the extent of myelination throughout the brain. By using this technique, one can also examine specific areas of the brain to see where most of the myelinogenesis occurred.

Instead of fixing the dissected brains using traditional fixatives, snap freezing for TEM research could be used. This would eliminate the possibility of membrane damage due to fixative procedures (Vigil *et al.*, 1984). Furthermore, proteomics could be used to specifically investigate myelin basic protein. This will indicate whether there is an increase in this protein. It would also show which other

proteins are being synthesized, which would indicate what other areas of the cell are also effected by digoxin.

Culture oligodendrocytes *in vitro* and confirm whether digoxin truly induces proliferation of this cell type.

Chapter 4:

Digoxin cytotoxicity *in vitro*, using the chick embryo model.

4.1. INTRODUCTION

Cytotoxicity testing is the method that estimates the ability of substances to kill cells, and that predicts how these substances will affect human beings; it is expected to replace whole animal toxicity testing which is complex, costly, time-consuming, and increasingly criticised by animal-welfare groups (Goldberg, 1989). Various different animal models are available for use in *in vitro* cytotoxicity studies.

The great advantage of using the chicken embryo model is the option of testing a hypothesis both *in vitro* and *in vivo*, or in the case of a chicken, *in ovo*, during development. *In vivo*, this animal model has been used to examine among others, the effect of rabbit sera on embryo susceptibility to septicaemia (Tieffenberg *et al.*, 1978), the effects of a human melanoma on the embryonal eye before maturation of the immune system (Luyten *et al.*, 1993), and various problems in developmental biology and teratology (Fineman and Schoenwolf, 1987). *In vitro*, this animal model has been used to examine the effects of among others, anti-metastatic drugs after introduction of human cancer cells (Gvosdjan *et al.*, 2004), virus production in chick embryo fibroblasts (Volkmann and Morgan, 1974), and aflatoxin B1-mediated cytotoxicity in chick embryo hepatocytes (Iwaki *et al.*, 1993). This model was chosen to examine digoxin cytotoxicity *in vitro*, because it is a well established animal model that is cost-effective and has the advantage of comparing the *in ovo* and *in vitro* experimental results.

Digoxin cytotoxicity has been studied in the human hepatoma cell line, HepG2. In this study researchers found that a 50% decrease in cell number was induced by a 50μM solution of digoxin. They also reported that there existed no dose-effect relationship and that higher concentrations of digoxin produced the same effect as that observed with 50μM digoxin (Tuschl and Schwab, 2004).

The following research question directed these experiments: How will digoxin influence the viability of chick embryo neurons *in vitro*?

4.2. MATERIALS

4.2.1. Chick embryos

Fertile Broiler Hatching eggs were obtained from National Chicks hatchery in Pretoria, South Africa. Eggs were stored at 4ºC until required for experiments. Eggs were never stored in excess of two weeks.

4.2.2. Reagents and media

Eagles Minimum Essential Medium (EMEM) powder, Hank's Balanced Salt Solution (HBSS) and Foetal Calf Serum (FCS) were purchased from Highveld Biological Company, Johannesburg, South Africa. Sartorius cellulose acetate membrane filters 0.22μm were purchased from National Separations, Johannesburg, South Africa. Fixatives, acids and organic solvents, such as gluteraldehyde, hydrochloric acid (HCl), acetic acid, isopropanol, and formic acid were analytical grade and purchased from Merck, Johannesburg, South Africa.

Streptomycin sulphate, penicillin G (sodium salt), Amphotericim B and Trypsin were obtained from Life Technologies Laboratory supplied by Gibco BRL

Products, Johannesburg, South Africa. Bovine Serum Albumin (BSA) was purchased from Boehringer Mannheim, Randburg South Africa.

Sodium hydrogen carbonate ($NaHCO_3$) was purchased from Merck, Johannesburg, South Africa. Digoxin powder, Crystal Violet powder and poly-L-lysine was puchased from Sigma-Aldrich, Atlasville, South Africa.

Water was double distilled and de-ionised (ddH_2O) with a Continental Water System and sterilized by filtration through a Millex 0.2µm filter. All glassware was sterilized at 121^0C in a Prestige Medical Autoclave (Series 2100).

4.2.3. Plastic ware

The 24 well and 96 well plates, $25cm^2$ and $75cm^2$ cell culture flasks, 10mL and 5mL pipettes, 15mL and 50mL centrifuge tubes were from NUNC™ supplied by AEC- Amersham, Johannesburg, South Africa.

4.3. METHOD

4.3.1. Cultivation technique

Fertile Broiler Hatching eggs were incubated in a Grumbach incubator at 37°C in humidified air for a period of 7 days to allow ample development and differentiation of tissues, i.e. neural tissue. The blunt ends of the eggs were swabbed with 70% alcohol to sterilize, after which the embryos were removed from the eggs and their brains removed through dissection.

Using scalpel blades and a Petri dish, the brains were cut into a fine pulp. This tissue was then transferred to a 50mL tube and washed three times with Hank's Balanced Salt Solution (HBSS) to remove excess blood and non-neuronal cells.

In order to separate cells further to obtain a single cell suspension, the tissue was then incubated in 0.025% trypsin for 10min in a CO_2 incubator. The trypsin was removed and the tissue immediately washed in Eagle's minimum essential medium (EMEM) containing 5% FCS to stop trypsination.

Ten millilitres of EMEM was added and the solution of medium and separated tissue repeatedly pipetted up and down in the 50mL tube to mechanically force a single cell suspension. The cell suspension was removed and incubated in a $75cm^2$ cell culture flask for a period of 1 hour. This was done to separate the fibroblasts from the neurons, because fibroblasts adhered to the cell culture flask surface whereas the neurons remained in suspension in the EMEM. While the neurons and fibroblasts were being separated 24 well plates were coated with Poly-L-lysine coated (1ml Poly-L-lysine in 9ml sterile ddH_20) for a period of 30 minutes.

The single cell suspension was then removed and cells were counted with a haemocytometer. EMEM was added to obtain a cell concentration of 8×10^4 cells/mL. Following this, 500µL of the cell solution was transferred to each well of a 24 well plate. The plate was then incubated at 37ºC and 5% CO_2 for two days before exposure.

All manipulations were done under sterile conditions in a laminar flow hood and all laboratory work was done in accordance with the ethical committee of the University of Pretoria.

4.3.2. Dosages

In a similar fashion as was used in the *in vivo* study *(Chapter 3)* the effect of high and low dosages on the cell number of chick embryo neurons in primary culture was determined. Digoxin in powder form was dissolved in ethanol and then

diluted in water to prepare two working stock solutions of 51.2µM and 102.4µM containing a final ethanol concentration of 60%.

4.3.2.1. Low dose digoxin

Plates in these experiments were organized into 3 groups of 8 wells each. The groups received the following dosages: controls (no exposure); 1.28nM (1.5% EtOH); and 2.56nM (3% EtOH). Cells were exposed for 24 hours. Experiments were done in quadruple.

4.3.2.2. High dose digoxin

Toxicity is a function of dosage and exposure time and therefore these experiments were conducted to examine the effect of a high concentration of digoxin would have on neuron viability, over time. Time intervals at which the cells were fixed are as follows: 5 minutes; 30 minutes; 1 hour; 6 hours; 12 hours; 24 hours; and 48 hours. Plates in this experiment were divided into 6 groups of 4 wells each. The different groups received the following amounts of the digoxin-EtOH solution: controls (no exposure); 12.8nM (7.5% EtOH); 15.4nM (9% EtOH); 19.2nM (11.3% EtOH); 22.4nM (13.1% EtOH); and 25.6nM (15% EtOH). Experiments were done in quadruple.

4.3.3. Crystal Violet (CV) Assay

To prepare the CV dye solution, 100mg of CV powder was added to 100mL of water. In this study the CV assay was chosen to evaluate cell number, as the addition of NR and MTT to viable neuron primary cultures leads to cellular detachment.

Following the desired incubation period for each experiment, 100µL of 11% gluteraldehyde prepared in water was added to each well of the 24 well plate and

the cells fixed for 30 minutes. The medium-gluteraldehyde solution was then removed and the wells left overnight to dry. For staining, 300µL of the CV solution was added to each well and the cells stained for 30 minutes, after which the CV solution was removed and wells washed with tap water to remove any excess stain. Again the plates were left to dry overnight. To extract the dye from the cells, 300µL of 10% acetic acid was added to each well and 100µL of the extracted dye solution was the transferred to a 96 well plate and read with a plate reader (Biotech ELx 800) at a wavelength of 570nm. Cell number in experimental groups is expressed as percentage of the absorbance measured in control groups (not exposed to drug).

4.4. RESULTS AND DISCUSSION

4.4.1. Low dose digoxin

An analysis of variance (ANOVA) was used to statistically analyse the results because the experiment included three independent groups of quantitative observations. At concentrations ranging from 1.28nM to 2.56nM, differences in cell number from 100% to104% was observed and these results were statistically significant with ***p<0.001***. See fig. 4.1.

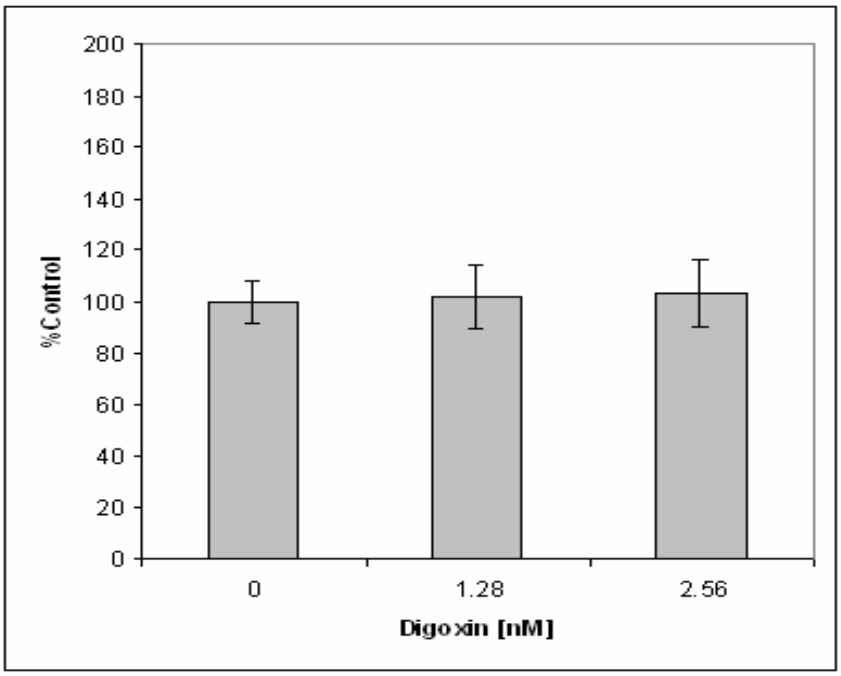

Fig. 4.1. Results obtained from CV assay that show the effect of low dose digoxin on neuron viability.

The crystal violet staining assay was developed by Saotome *et al.* in 1989 for evaluating the cytotoxicity of chemicals such as drugs for injection. Two of the advantages of the CV staining method over other cytotoxicity tests are that, after the staining, the morphological changes in fixed cells are observable any time by microscopy and the tested microplates can be stored long-term for reference purposes. The CV molecule consists of three carbon rings, which are connected centrally by a single carbon atom. Peripherally a $N(CH_3)_2$ molecule is attached to each carbon ring (see fig. 4.2). The CV molecule is a cation and therefore binds avidly to negatively charged particles in the cytoplasm. This includes the negatively charged phosphate backbone of RNA and DNA and the carboxyl groups of proteins.

CV staining is used to indirectly measure cell number. The chick embryo neurons in cell culture are differentiated cells that do not have the ability to divide nonetheless a significant increase in CV uptake occurred in the cells across the

increasing dosages with ***p<0.001***. Furthermore there is no scientific literature that supports the theory that digoxin exposure results in cell proliferation and from the previous chapter it is clear that digoxin induced cell death *in vivo*, not proliferation. Therefore an increase in absorbency can only be ascribed to an increase in RNA and protein content that is usually associated with protein synthesis. However, digoxin is a steroid-like structure, which means it can readily cross the plasma membrane and literature shows that digoxin inhibits protein synthesis through binding directly to ribosomes forming an inactive complex (Paszkiewicz-Gadek *et al.*, 1988). Even though digoxin does not directly increase protein synthesis, it causes an intracellular increase in Ca^{2+}, which has been shown to modulate protein synthesis on several different levels such as rapid initiation of translation (Brostrom *et al.*, 1983; Chin *et al.*, 1987).

Although direct evidence for the inductive effect of digoxin on protein synthesis is not clear from the literature, it is very clear when studying the previous chapter that myelination of the CNS cannot occur in the absence of protein synthesis and therefore, digoxin must have had a stimulatory effect on protein synthesis, *in ovo*, most probably through increasing the levels of $[Ca^{2+}]_i$, simply because no CNS myelination was seen in any of the control sample population.

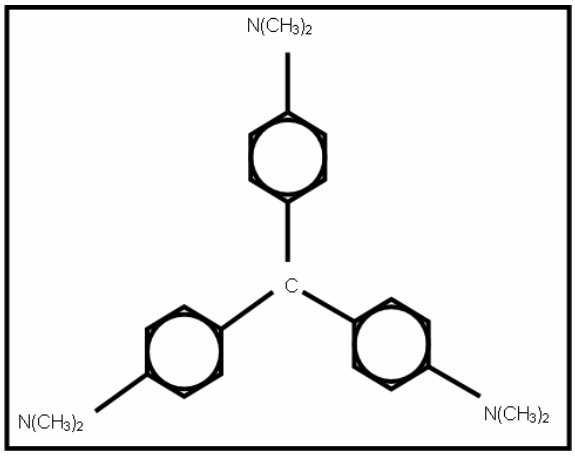

Fig. 4.2. The molecular structure of crystal violet dye.

Another group of proteins that are known to be synthesized and increase cytosolic protein content following cellular stress is called heat shock proteins (HSP). The different types of stresses that they are known to react to include, amongst others: anoxia, ischemia, surgical stress, viral agents and EtOH. In the literature these molecules have been referred to as molecular chaperones. This terminology is derived from their function of associating with denatured proteins and assisting with either the repair or degrading, following stress injury (Whitley *et al.*, 1999). In this experiment, 1.5% and 3% EtOH was present in the 1.28nM and 2.56nM digoxin concentrations, respectively. The increase that was seen can be the result of increased cytosolic heat shock protein content brought on by cellular stress induced by the EtOH exposure. However, more recent research has shown that the cardiac glycoside, ouabain, decreased the mRNA content of the 70kDa HSP in cardiac myocytes, following 8 hours exposure (Neuhofer *et al.*, 2002). In this experiment however, the cells were exposed to a different cardiac glycoside (digoxin) and for a longer period and therefore one cannot completely exclude HSPs as the cause for increased cytosolic protein content.

Therefore, from the first section of this experiment, it was concluded that as digoxin concentration increases to ≈2.5nM, it has an almost linear stimulatory effect on protein synthesis in neurons. This is possibly an indirect effect on the neuronal tissue that occurs through increasing the levels $[Ca^{2+}]_i$ by inhibiting the function of the membrane-bound enzyme, Na^+/K^+-ATPase, but further research is required to confirm the stimulatory effect of the elevated $[Ca^{2+}]_i$.

4.4.2. High dose digoxin

The second section of the experiment used higher dosages of digoxin to examine what effect these dosages will have on neurons and a second factor time was included. Up to 12 hours exposure, absorbance decreased to reach the lowest value of 81% of control (no drug added), after which, absorbance increased to and peak value of 111% of control values. These results are given in fig. 4.3.

ANOVAs were applied in two directions: first with ***I*** defined by concentrations (table 4.1.) and second with ***I*** defined by time intervals (table 4.2.).

A

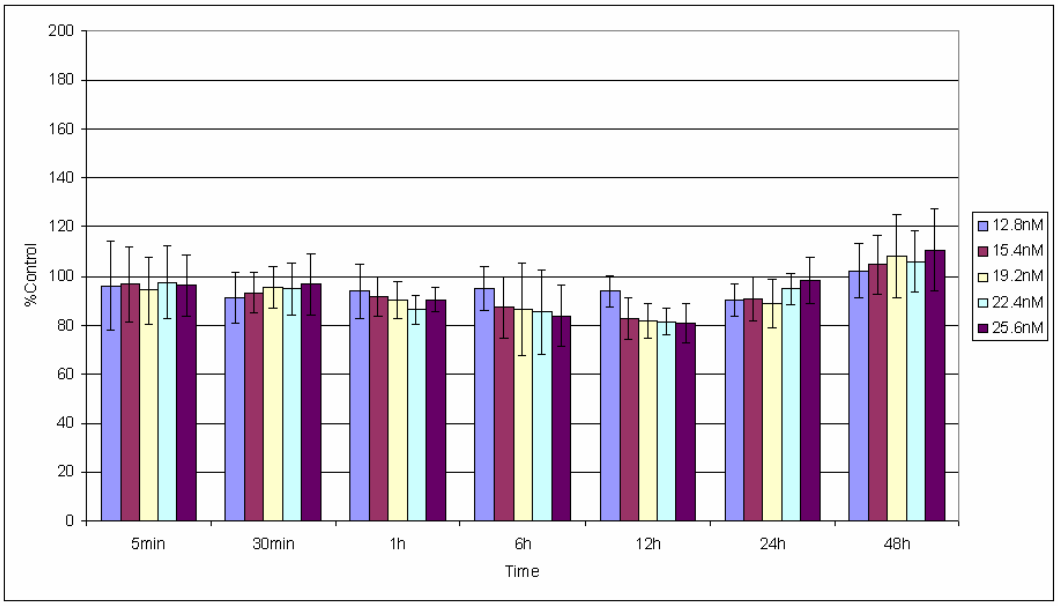

B

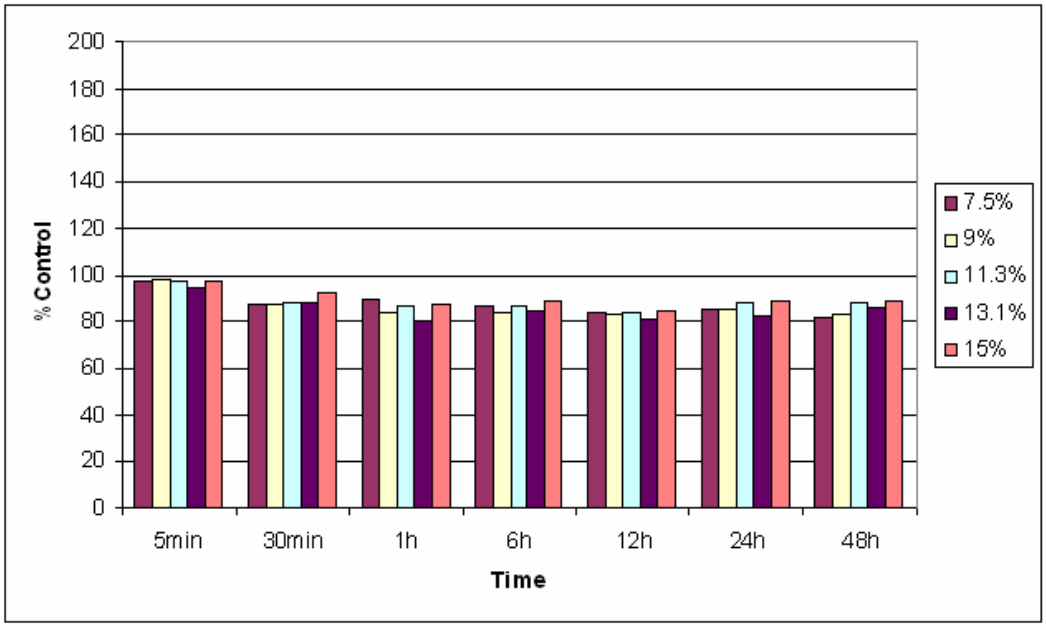

Fig. 4.3a Pooled results of the high dose exposure over time presented as a percentage of the control (no drug added). All results shown are statistically significant. Controls (not shown) equal 100%.
Fig. 4.3b. Results obtained from the control experiment, cells exposed to EtOH alone.

This experiment was repeated with EtOH alone, which acted as carrier molecule in the digoxin experiments. EtOH concentrations were the same as in the digoxin experiments. It was found that EtOH exposure resulted in a slight decrease in cell number up 30 minutes of exposure, after which CV assay results remained similar.

4.4.2.1. ANOVA with *I* = concentrations

In the first ANOVA application, the independent groups ($\boldsymbol{I}$) was defined by the different concentrations of digoxin. An ANOVA was carried out for every time interval. All time intervals were shown to be highly statistically significant across the whole dosage range, as shown in table 4.1. The ANOVA was performed twice for each $\boldsymbol{I}$. Once with and once without the control values obtained from the CV assays. The controls were excluded from the ANOVA in order to probe for any significant differences that might have occurred between the different dosages alone. When the controls were excluded from the ANOVA, none of the time intervals differed significantly except for exposure times of 12 hours and 24 hours, which were highly significant. These results are also given in table 4.1. $\boldsymbol{S_{pooled}}$ represents the standard deviation across the independent groups.

Table 4.1. ANOVA results for time intervals across dosage range. *I* defined by concentrations.

Dosage	*p*-value	S_{pooled}	*p*-value (controls excluded)
5min	<0.001	0.033	0.999
30min	<0.001	0.022	0.877
1h	<0.001	0.041	0.19
6h	<0.001	0.028	0.659
12h	<0.001	0.023	**<0.01**
24h	<0.001	0.06	**<0.01**
48h	<0.001	0.08	0.632

As mentioned above, the ANOVAs across the dosages with $\boldsymbol{I}$ defined as time intervals were all highly significant with ***p<0.001*** (table 4.1.). Interpreted, this means that at all time intervals, the dosages had a significant effect on the

neurons' CV results when compared to control values. Differences between controls and dosages up to 12 hours are the result of cell death because CV absorbance results gradually decreased. The cell death most probably still continued after 12 hours. The increase in CV absorbance results seen after 12 hours must be the result of protein synthesis (refer to section 4.4.1.) because chick embryo neurons are unable to divide and cell death is probably still occurring.

In order to compare only the different dosages to each other, these ANOVAs were also performed with control values excluded. This was done to probe for significant differences between different the dosages applied in this section experiment. Table 4.1 shows that when controls were excluded, significant differences between dosages was only detected at 12 and 24 hours exposure. This is indicative of the some dosages exerting their effect on the cells faster than other dosages. The higher dosages probably exerted their effect faster than the lower dosages because more digoxin would inhibit more Na^+/K^+-ATPase, which would increase $[Ca^{2+}]_i$ faster and resultantly induce both cell death and protein synthesis more rapidly. This by itself could also serve as evidence for the increased protein synthesis, seeing that this is the only explanation for the significant differences detected at 12 and 24 hours exposure.

No significant difference was detected between the dosages at 48 hours exposure. This is most probably because protein synthesis has reached a saturation level after this period of exposure because a limited amount of nutrients are present in the medium. No medium changes were performed. This could not be the cessation of protein synthesis because of cell death because the cell membrane would have ruptured causing leakage of the CV dye when it's extracted.

4.4.2.2. ANOVA with *I* = time intervals

In the second ANOVA application, I was defined by the different time intervals of exposure. In this case, an ANOVA was carried out for every dosage. All dosages showed statistical significance, except for controls, as shown in table 4.2. S_{pooled} represents the standard deviation across the independent groups.

Table 4.2. ANOVA results for dosages across time. I defined by time intervals.

Dosage	*p*-value	S_{pooled}
Controls	0.95	0.086
12.8nM	<0.05	0.052
15.4nM	<0.001	0.022
19.2nM	<0.001	0.025
22.4nM	<0.001	0.023
25.6nM	<0.001	0.023

Control absorbance values decreased over time but this was not shown to be statistically significant with ***p=0.95***. Interpretation of this is that the decrease in absorbance seen in the exposed groups is not the result of any factor other than the investigational product because all exposed groups were statistically significant. The significance of dosages under 15nM was borderline with ***p=0.048*** and dosages over 15nM were highly significant with all dosages showing ***p<0.001***.

When examining the end result of the CV assays, the percentage of control values (PCV), it shows that the PCV slowly decreased over time until it reached a low at 12 hours of exposure, after which the PCV increased up to 48 hours exposure. The decrease in PCV can be attributed to cell death. This correlates with results from the previous chapter, which show that digoxin exposure *in ovo* induced cell death. It could also be explained by decreased protein synthesis. However, this is not likely when recalling the discussion on the low dose arm of this experiment *(section 4.4.1.).* One could argue that the high volumes of EtOH may have induced the cell death and not the digoxin exposure but an experiment

was performed with EtOH alone that showed the small effect that EtOH had on the CV assay results.

The increase in PCV from 12 hours up to 48 hours exposure could not be the result of cell proliferation. First, because cell death occurred up to 12 hours (and probably continues after) and second, because neurons are non-dividing cells. The increase in PCV could once again be explained by increased protein synthesis. Because digoxin has been shown to inhibit protein synthesis (Paszkiewicz-Gadek *et al.*, 1988), the increase in protein synthesis is probably the result of increased $[Ca^{2+}]_i$. This correlates with the increase in PCV only occurring after 12 hours. First, digoxin has to initially exert its action on Na^+/K^+-ATPase for $[Ca^{2+}]_i$ to increase up to a specific threshold level before it can induce protein synthesis. After this, protein synthesis itself takes up time and then enough protein must be synthesized to alter the CV assay results.

4.6. CONCLUSIONS

Conclusions that can be drawn from this experiment are:

1. Digoxin at dosages of ≥1.3nM induces protein synthesis in neuronal tissue *in vitro*, most probably indirectly through increasing $[Ca^{2+}]_i$.

2. The higher the dosage of digoxin, the faster its stimulatory effect on protein synthesis would occur. As the dosage of digoxin increases to ≈2.5nM an almost linear increase in the stimulatory effect on protein synthesis would occur.

3. At dosages above 13nM, digoxin induces cell death of neuronal tissue *in vitro*. However, this concentration may be lower.

4. Dosages above 15nM have a greater effect of cell damage on neurons than dosages below this value.

5. *In vitro*, digoxin-induced protein synthesis in neurons reaches a saturation level, given that no medium changes are performed.

4.7. FUTURE RESEARCH

To further study the effect of digoxin on protein synthesis, the same experiments can be repeated under the same conditions and the effect on protein synthesis can be determined using ^{35}S-methionine labelling with scintillation counting (to determine levels) and two dimensional gel electrophoresis (to identify specific proteins). One can also examine whether therapeutic dosages has a similar effect on protein synthesis.

To confirm that the protein synthesis is induced by $[Ca^{2+}]_i$, one could use a Na^+/Ca^{2+}-exchanger blocker, which would block $[Ca^{2+}]_i$ increase directly caused by the increased $[Na^+]_i$ resulting from Na^+/K^+-ATPase inhibition. If protein synthesis does not take place, it must be induced by Ca^{2+}, if it still occurs it's either the direct result of digoxin or induced through another indirect pathway, for example increased $[Na^+]_i$.

Also, to see if the saturation point reached at 48 hours is the result of limited nutrients, one could change the medium after 24 hours.

To confirm cell death, this experiment has to be correlated with another viability assay.

Chapter 5:

Fluorescence microscopic examination of digoxin cytotoxicity *in vitro*, using the chick embryo model.

5.1. INTRODUCTION

Propidium iodide (PI) is a polar molecule and cannot readily cross cellular membranes. Therefore, PI is excluded from cells where membrane integrity is not compromised. Once cellular membranes such as the plasma membrane have sustained damage, PI can enter the cell and will bind to the negative backbone of the DNA. PI is a stable fluorescent dye which absorbs blue-green light at 493nm and emits a bright red fluorescent colour at 630nm. PI is non-toxic to neurons and is therefore widely used as an indicator of neuronal membrane integrity and cell damage. (Pozzo *et al.*, 1994; Bauer *et al.*, 2006)

Because of the fact that PI binds to the negative backbone of the DNA helix, it has been used in previous studies to visualize and assess changes in nuclear morphology (Yeh *et al.*, 1981; Ahlbom *et al.*, 1999; Black *et al.*, 2004). In these studies researchers have studied both the apoptotic and necrotic mechanisms of cell death using PI staining. When PI penetrates the cell to bind to the DNA backbone, it is already clear that that particular cell has lost the integrity of its plasma membrane. This, in itself, is indicative of necrosis or oncosis (cellular swelling). However, PI can also cross the plasma membrane in cells that are in the late stages of apoptosis. To distinguish between necrosis and apoptosis when using PI staining, one must look at changes that occurred in the nuclear morphology of these cells.

Therefore, this experiment aims to answer the following research question: What type of cell death is indicated by nuclear morphology, following digoxin exposure?

5.2. MATERIALS

5.2.1. Chick embryos

Fertile Broiler Hatching eggs were obtained from National Chicks hatchery in Pretoria, South Africa. Eggs were stored at 4ºC until required for experiments. Eggs were never stored in excess of two weeks.

5.2.2. Reagents and media

Potassium chloride (KCl), potassium dihydrogen phosphate (KH_2PO_4), disodium hydrogen phosphate (Na_2HPO_4) and sodium chloride (NaCl) were purchased from Merck, Johannesburg, South Africa. Propidium iodide (PI) was obtained from Sigma-Aldrich, Atlasville, South Africa.

5.2.3. Plastic ware

The 6 well plates, 25cm^2 cell culture flasks, 10mL and 5mL pipettes, 15mL and 50mL centrifuge tube, micro centrifuge tubes were purchased from NUNC^{TM} supplied by AEC- Amersham, Johannesburg, South Africa.

5.3. METHOD

5.3.1. Culturing technique

Primary chick embryo neurons were cultured as described in *Chapter 4, section 3.3.1.*, but the neurons were cultured in 6 well plates instead of 24 well plates.

Also, microscopy cover slips were placed at the bottom of each well before the wells were coated with poly-L-lysine. Neurons and medium (3mL) were then added to each well and the neurons monolayer developed on top of the cover slip. The primary culture was allowed to develop for a period of 2 days before exposure for 24 hours.

5.3.2. Dosages

Cells were exposed to a 53nM (1.3% EtOH) digoxin solution for approximately 1.5 hours to induce cell death. Controls were not exposed to any substance. The experiment was done in duplicate.

5.3.3. Fluorescence microscopy

The PI solution was prepared by adding 1mg of PI powder to 1mL ddH_2O. Dulbecco's phosphate buffer solution (DPBS) stock solution with pH 7.4 was prepared by dissolving 2g/L KCl, 2g/L KH_2PO_4, 80g/L Na_2HPO_4 and 80g/L NaCl in 1L ddH_2O.

Medium was removed from each well and then well washed with DPBS (1:10 dilution). A volume of 1.2mL of DPBS and 30µL of PI solution were added to each well and the plate left in a dark room for 5 minutes. Following this, the PI/DPBS solution was removed from each well and enough DPBS added to cover the bottom of each well. The exposed neurons were then examined under a Zeiss Axiovert 200 fluorescence microscope (Carl Zeiss Werke, Göttingen, Germany). Micrographs were taken by a Zeiss Axiocam MRc5 digital camera (Carl Zeiss Werke, Göttingen, Germany).

5.4. RESULTS AND DISCUSSION

Many observable differences exist between the morphological features of apoptosis and necrosis. Necrosis is normally the result of extreme variations from normal physiological conditions such as hyperthermia and hypoxia that result in damage to the plasma membrane. Necrosis is the result of the cell losing its ability to maintain homeostasis, which causes the influx of extracellular ions with associated water influx (osmosis). Signs of necrosis include swelling of the organelles, specifically the mitochondrion and cytoplasm. Necrosis ends with rupturing of the plasma membrane and disintegration of organelles, with subsequent leakage of cellular contents into the extracellular space, which leads to an inflammatory response (Roche Applied Sciences, 2007).

Apoptosis, on the other hand, is programmed cell death and occurs under normal physiological conditions. Apoptosis starts with aggregation and marginalisation of the nuclear chromatin and shrinkage of both the nucleus and cytoplasm, as opposed to swelling in necrosis. Organelles, such as the mitochondrion, remained intact. Another sign indicative of apoptosis is that of blebbing of the plasma membrane, which is associated with the cytoplasmic shrinkage. Apoptosis ends with fragmentation of the cell into various apoptotic bodies which may contain intact organelles. Fragmentation is the result of individual blebs dissociating from the rest of the original cellular body, thus forming an apoptotic body. *In vivo*, these apoptotic bodies are easily recognised and phagocytised, in this way preventing an inflammatory response (Roche Applied Sciences, 2007). The main morphological features are summarised in table 5.1.

Table 5.1. Main morphological differences between necrosis and apoptosis.

NECROSIS	APOPTOSIS
Cellular swelling	Cellular shrinkage and blebbing
Disintegration of organelles	Organelles remain intact
Loss of membrane integrity	Marginalisation of nuclear contents

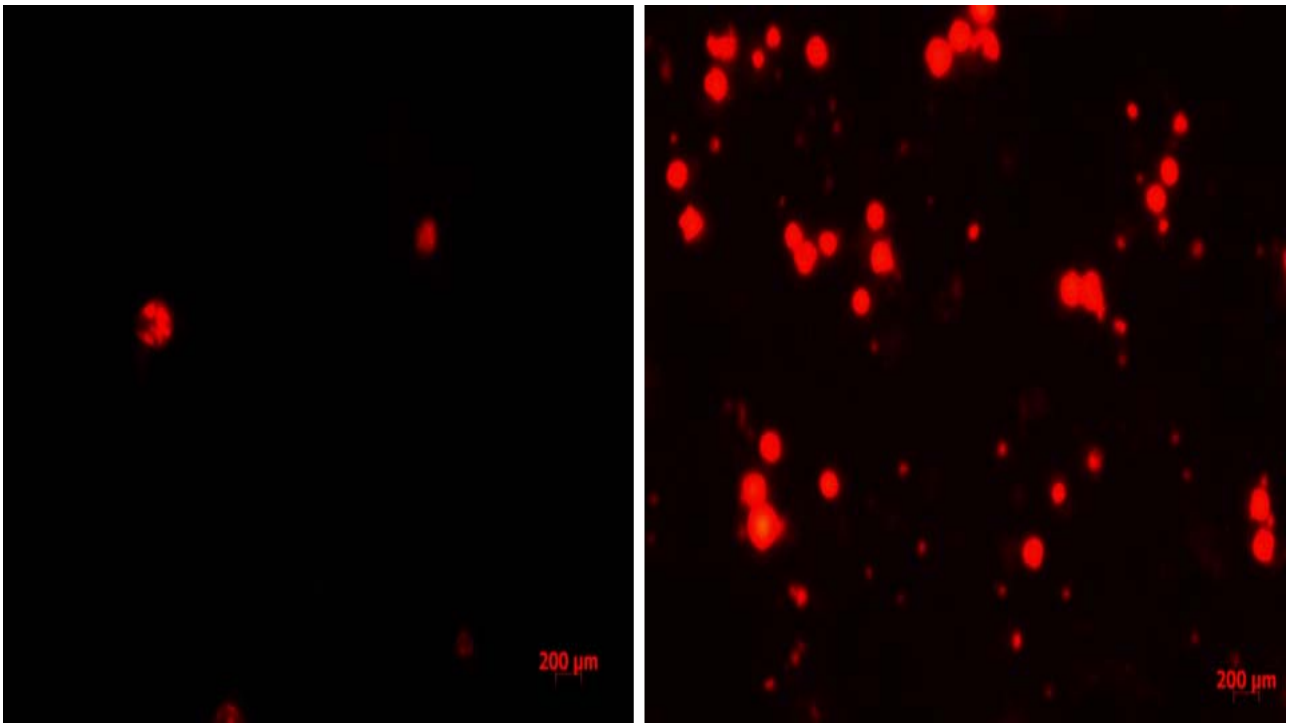

Fig. 5.1. Fluorescence micrograph of controls (left) as compared to cells exposed to 53nM digoxin (right). Cells were stained with PI indicating the damaging effect that digoxin has on the plasma membranes of neurons.

Cells in this experiment were exposed to 53nM digoxin (1.3% EtOH) and were then stained with PI for a period of 5 minutes. Fig. 5.1 shows the cells that absorbed the PI stain. When comparing the micrographs of the controls and experimental cells, it is clear that digoxin exposure resulted in a dramatic increase in PI uptake into the cells. This is an indication of plasma membrane damage caused by digoxin seeing that PI cannot penetrate cells with intact membrane morphology because of the fact that PI is a polar molecule (Pozzo *et al.*, 1994; Bauer *et al.*, 2006). This is consistent with what was seen with EM in *Chapter 3*, confirming the conclusion that necrosis would be the main mode of cell death.

However, contradicting results to this were found in the form of condensation of the nuclear chromatin. The arrows in fig. 5.2a show two cells in which condensation of the nuclear contents is visible. Nuclear chromatin condensation is indicative of apoptosis. These results are consistent with the results of the low dose section of the experiment in *Chapter 3* in which the EM results suggested that the cells exposed to a low dosage of digoxin were not dying of either apoptosis or necrosis alone, but of a combination of the two called aponecrosis. Chromatin condensation is again visible in fig. 5.2b that shows the nucleus of a cell in which half of the nucleus shows normal morphology while nuclear chromatin condensation has started the other half. In this particular cell apoptosis is not that advanced yet because half of the nucleus shows normal morphology. This means that the PI that entered the cell must be as a result of oncosis/necrosis.

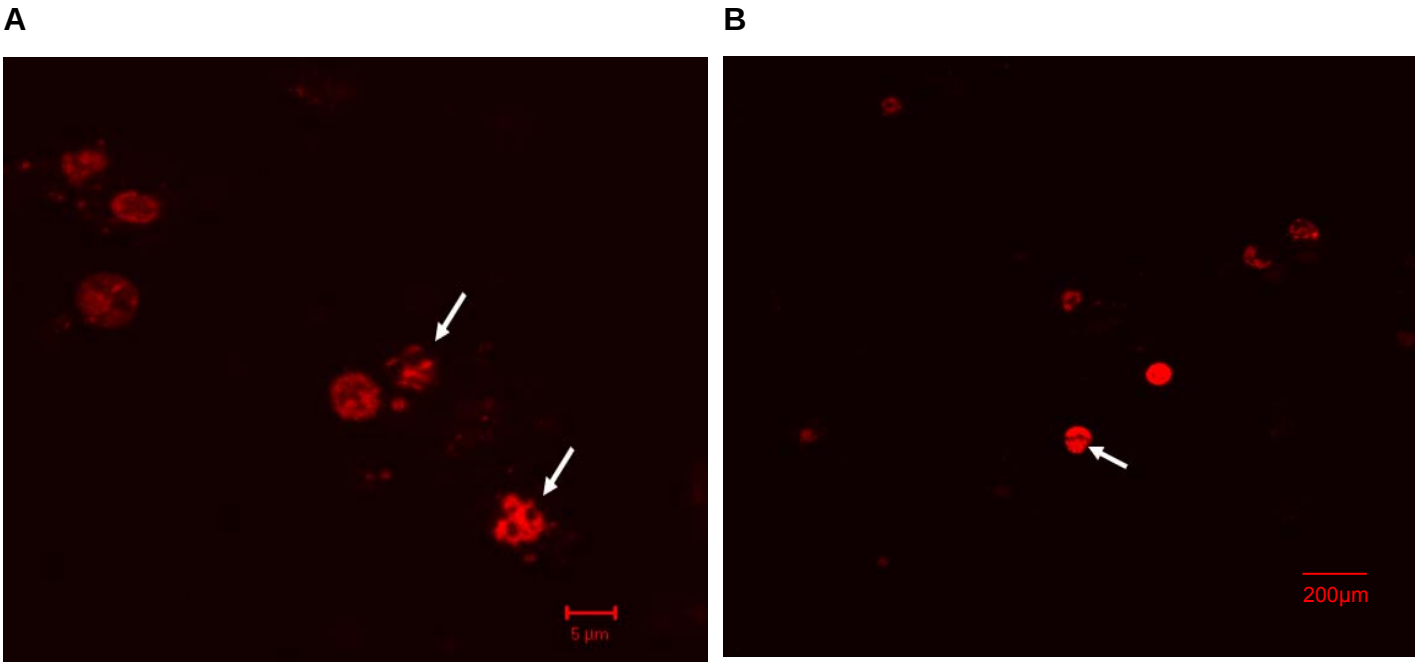

Fig. 5.2. (A) Fluorescence micrograph of cells stained with PI, indicating disrupted nuclear morphology (arrows). **(B)** Nucleus of a cell undergoing nuclear chromatin condensation (arrow).

More evidence for cell death by means of apoptosis was found in the form of marginalisation of the already condensed nuclear chromatin. Fig. 5.3 was chosen because it demonstrates marginalisation of the nuclear contents, indicated by the arrows. On the contrary, this figure also shows disintegrating cellular contents, which can be seen inside the dashed oval.

Signs of both apoptosis and necrosis were seen when studying nuclear morphology using PI staining, which is consistent with the results obtained from the experiment in *Chapter 3*. At this concentration, digoxin induces not apoptosis or necrosis alone but result in cell death in a hybrid mechanism, aponecrosis. The chosen method has the advantage of being cost-effective and relatively easy to perform, but has the limitation in that this method is qualitative and not quantitative. However, this method was chosen because it only needed to confirm the results obtained in *Chapter 3*, and not any more detail such as the ratio of cells in apoptosis *versus* cells in necrosis.

Not much literature is available with regards to digoxin exposure and PI staining, which seriously compromises a comparison with other studies. The only study found states that researchers have demonstrated with PI staining that digoxin is the most detrimental concerning damaging of cellular membranes when compared to paracetamol, isoniazid, paraquat, 2,4-dichlorophenoxy acetic acid and malathion (Tuschl and Schwab, 2004). In this study, PI was able to penetrate the bulk of the cells exposed to digoxin, which also indicates the damaging effect that digoxin has on cellular membranes, specifically the plasma membrane.

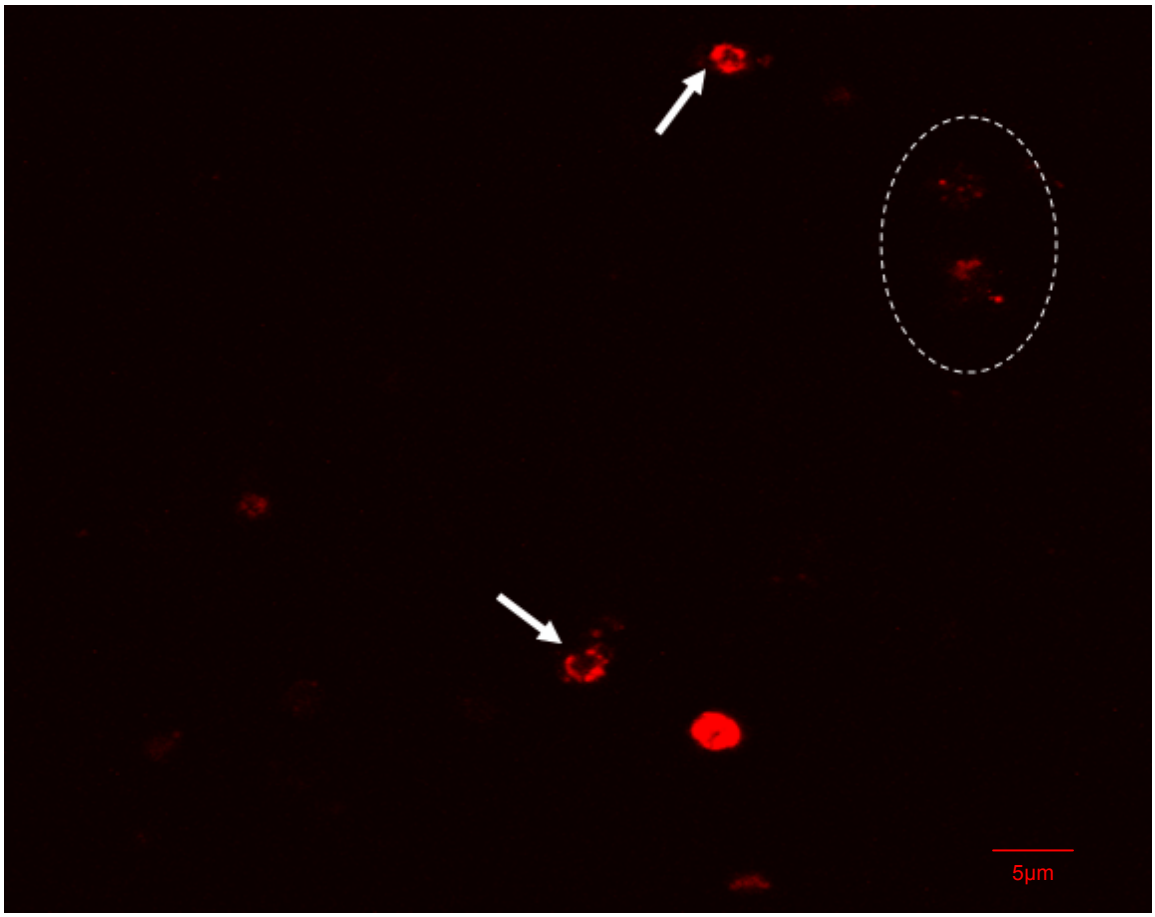

Fig. 5.3. PI staining shows marginalisation of nuclear contents (arrows). This is generally a sign of apoptosis. On the contrary, disintegrating cellular contents can be seen inside the dashed oval.

Other dyes that can be utilised to stain nuclear material to study morphology are the Hoechst stains (33342 and 33258) and 4',6-diamidino-2-phenylindole (also known as DAPI) (Norton and Atherton, 1998; Ichinose *et al.*, 2003). These stains also bind to DNA and are capable of readily passing through cellular membranes. For this reason, these stains are often used to study nuclear morphological changes that occur during apoptosis because plasma membrane integrity remains intact during apoptosis and other stains such as PI cannot penetrate these cells. This is why these other dyes were not chosen for the present experiment because one would not be able to assess the amount of damage that has occurred to the plasma membrane. If the other stains were used the results would have been interpreted as apoptosis occurring and not aponecrosis.

5.5. CONCLUSIONS

Conclusions that can be drawn from this experiment are:

1. Cells exposed to a digoxin-EtOH solution undergo aponecrosis as the micrographs in this chapter indicated signs of both mechanisms of cell death. An aponecrotic state is reached at concentrations of 53nM (1.3% EtOH) with exposure time of 1.5 hours. This confirms the conclusion made in *Chapter 3* stating that digoxin induces aponecrosis.

5.6. FUTURE RESEARCH

Rhomadine 110 derivatives and 4-methoxy-2-napthylamide are two examples of fluorescent probes that detect viability through intracellular enzyme activity (CellProbe™ Reagents: An Introduction), that can additionally be used to allow one to study not only nuclear morphology but also cellular viability. Flow cytometry would most probably be the best way to assess cell viability using the fluorescent probes Annexin V and PI, because flow cytometry can quantify both

cellular viability and cell volume. Flow cytometry with Annexin V and PI staining have extensively been used in the literature to study the ratio of apoptosis *versus* necrosis occurring in various cell types following different exposures. In the brain it been used to examine cell death following hypoxic insults (Jung *et al.*, 2006), differences in hydrostatic pressure (Agar *et al.*, 2006), β-amyloid exposure (Huang and May, 2006), and Ca^{2+} transients (Schroter *et al.*, 2005) to name a few.

Chapter 6:

Concluding discussion

6.1. APONECROSIS

6.1.1. Hypothesis concerning aponecrosis

Aponecrosis is a relatively novel concept seeing that very little literature is available that describes this combined mechanism of cell death. This mechanism of cell death has been described in both brain and liver tissue (Cheng *et al.*, 2003; Pretorius and Bornman, 2005).

In liver tissue, hepatotoxicity was induced by a substance known as paraquat, which uses intracellular oxygen to initiate superoxide and subsequent reactive oxygen species (ROS) generation. ROS induced aponecrosis in *gpx1* knockout mice (Cheng *et al.*, 2003). *Gpx1* encodes for glutathione peroxidase-1, a selenium-dependant anti-oxidant. Previous research indicates that decreased availability of reduced glutathione, the primary co-substrate for glutathione peroxidase, potentiates the effect of hydroperoxide oxidant stress on receptor-operated Ca^{2+} entry across the plasmalemma and Ca^{2+} release from internal stores (Elliott *et al.*, 1995). In brain tissue, aponecrosis was induced by estrogenic-chemical induced neurotoxicity. This neurotoxicity was mediated by intracellular Ca^{2+} levels (Pretorius and Bornman, 2005).

It is a well-known fact that digoxin increases intracellular Ca^{2+} levels by inhibiting the membrane sodium pump, Na^{+}/K^{+}-ATPase. This digoxin-induced increase in

$[Ca^{2+}]_i$ could explain the aponecrosis seen in *Chapters 3 and 5*. It should be noted that in both cases where aponecrosis was detected in this current study, the cells were exposed to low doses of digoxin. It should also be noted that when low doses (1.28nM - 2.56nM) and high doses (12.8nM - 25.6nM) of digoxin is referred to in this discussion, the doses are still very high when compared to the therapeutic index of digoxin, which is 0.5-2ng/mL (Qasqas *et al.*, 2004; DIG, 1996; Eichhorn and Gheorghiade, 2002; Datta and Dasgupta, 2004).

Theoretically, digoxin is capable of inducing both apoptosis and necrosis through elevating $[Ca^{2+}]_i$. This was discussed in the literature review (*section 2.4.2.2*) where MPT is the formation of pores in the mitochondrial membranes and may be due to normal physiological conditions but become permanent after an injurious insult such as Ca^{2+} overload within the cell (Crompton, 1999; Bernardi, 1999; Lemasters *et al.*, 1998). MPT may result in apoptosis because the intermembranous space of the mitochondrion contains many killer molecules, such as cytochrome C and apoptosis inducing factor (AIF) (Pretorius and Bornman, 2005). Necrosis can also be induced in many different ways. The increase in $[Ca^{2+}]_i$ causes an increase in osmotic pressure across the plasma membrane, which results in the influx of water into the cytosol (cellular swelling). This increases the intracellular pressure and resultantly causes rupture of the plasma membrane. Ca^{2+} directly activates several isoforms of phospholipases, which also cause membrane damage in various organelles in the cytosol such as the nucleus and mitochondrion as well as the plasma membrane itself.

The high dose experiment using ultra-structural morphology (*Chapter 3*), showed that cell death was by necrosis. With this taken into account, one can speculate that low doses of digoxin (1.28nM - 2.56nM) cause apoptosis and that high concentrations (12.8nM - 25.6nM) cause necrosis and what is seen in this study as aponecrosis is the transition between the dosage-related types of cell death. It could be speculated that low doses of digoxin cause a mild but significant enough increase in $[Ca^{2+}]_i$ to result in cell death. If the $[Ca^{2+}]_i$ increase is mild

enough to cause MPT and not to damage the mitochondrion to the degree of dysfunction, apoptosis can occur, seeing that this mechanism of cell death is energy-dependent. On the other hand, high doses of digoxin would cause a severe increase in $[Ca^{2+}]_i$ that would cause both MPT and mitochondrion dysfunction. This will induce cell death by necrosis because cellular energy production has ceased and no energy is available for apoptosis. If this is true, low dose digoxin would cause apoptosis and high dose digoxin would cause necrosis. This is speculation because the necrosis seen in the aponecrosis could well just be the effect exerted by EtOH and *visa versa*.

The question that arises is whether aponecrosis is indeed a mode of cell death. Ultimately, the moment of cell death occurs through either apoptosis or necrosis. Rather, it is suggested that aponecrosis is an event that may occur during cell death but not a mechanism of cell death.

6.1.2. Future research concerning aponecrosis

Because of the fact that EtOH may play a role in the cellular death documented in this study, it needs to be eliminated from the investigational product. Digoxin as a molecule is hydrophobic and therefore needs a solvent as carrier in an aqueous matrix or medium. This problem can be solved by changing the investigational product to another molecule that induces the same increase in $[Ca^{2+}]_i$. One such molecule that increases $[Ca^{2+}]_i$ in an almost identical way is Melettin. Melettin, a peptide, is the main component present in bee venom. Melettin increases $[Na^+]_i$ by inhibiting Na^+/K^+-ATPase, which reverses the action of the Na^+/Ca^{2+}-exchanger and results in elevated levels of $[Ca^{2+}]_i$. Melettin has actually been shown to have a greater inhibitory effect on the membrane sodium pump than ouabain (Chen and Lin-Shiau, 1985).

The difference between melettin and digoxin, is its unique properties provided by its molecular structure. Melettin has both hydrophilic and hydrophobic termini,

which gives the molecule an amphipathic character (Mufson *et al.*, 1979). This provides the opportunity to examine the effects of increased $[Ca^{2+}]_i$ alone, without any external factors that might play a role in cell death such as a solvent carrier for the investigational product (EtOH in the current study).

Using Melettin to exert a similar effect to that of digoxin, one can examine the effect that an increase in $[Ca^{2+}]_i$ alone has on the mode of cell death. In this thesis I hypothesize that a certain threshold $[Ca^{2+}]_i$ level exists that determine whether a cell will die as a result of apoptosis or necrosis. Below this threshold, cell will die as a result of apoptosis. Above this threshold, cells will die as a result of necrosis, with the exception that at concentration values just above this threshold level, the dying cells will initially exhibit signs of apoptosis but will ultimately die as a result of necrosis. This event of necrosis with initial signs of apoptosis defines the phenomenon known as aponecrosis. The threshold $[Ca^{2+}]_i$ level differs for different tissue types.

To test this hypothesis, Melettin can be used at differing concentrations to examine when apoptosis alone occurs. The same can be done for necrosis alone. Probably the best way in which to do this are by means of flow cytometry, labelling the cells with two markers for apoptosis, such as Annexin V and two necrosis markers, such as the fluorescent DNA dye SG. Lemarie *et al.*, 2006 have recently described this technique to distinguish between apoptotic and necrotic cells. This will give an approximation of the value of this threshold level.

To better specify this level, a marker of mitochondrial function can be used, particularly because apoptosis is energy-dependent. The best mitochondrial area to measure for mitochondrial functioning is the electron transport chain (ETC). By measuring the ETC enzyme activity through blue native polyacrylamide gel electrophoresis (BN-PAGE), functional changes in the mitochondria can be evaluated (Jung *et al.*, 2000). By applying BN-PAGE on cells that have been exposed to increasing concentrations of melettin, the concentration of melettin

where mitochondrial function ceases could theoretically be determined. However, once these melettin concentrations and exposure times have been determined, it could be repeated and the cytosolic Ca^{2+} concentration measured to determine the threshold $[Ca^{2+}]_i$ level. Cytosolic Ca^{2+} measurement will not be discussed as this is a dissertation and not a protocol, but the main strategy on how to answer these questions is clear. The basic expected result from this study is graphically illustrated in fig. 6.1.

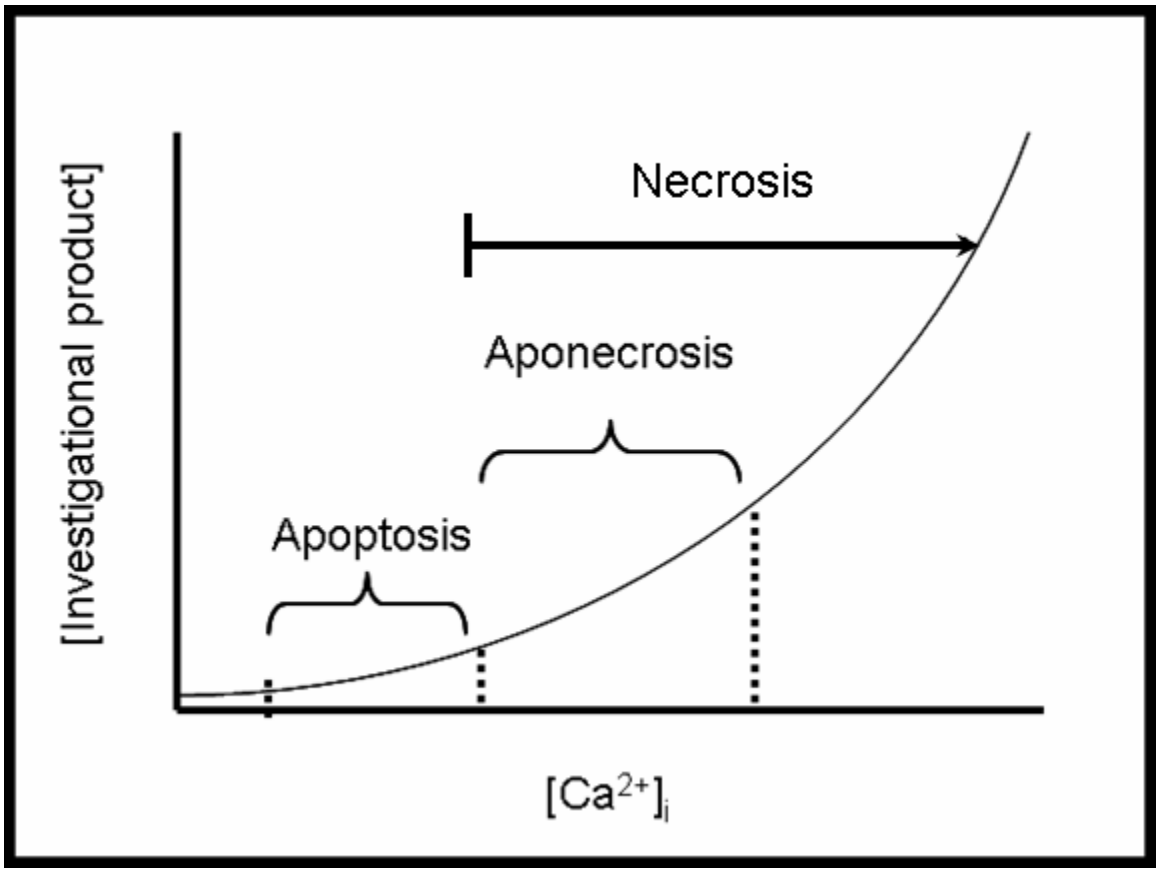

Fig. 6.1. Graphical illustration of expected result of the future research on aponecrosis. $[Ca^{2+}]_i$ increases exponentially, because Ca^{2+} influx causes a great release of Ca^{2+} from intracellular stores.

6.2. PREMATURE MYELINOGENESIS

6.2.1. Hypothesis concerning premature myelinogenesis

The high dose experiment in *Chapter 3* showed premature myelinogenesis. Myelinogenesis cannot occur without increased protein synthesis, which was confirmed with the high dose experiment (15.4nM -25.6nM digoxin) in *Chapter 4*. The specific structural protein that needs to be synthesized during myelinogenesis is myelin basic protein or MBP. Quakingviable (qk^v) mutant mice exhibit homology for a recessive genetic lesion that affects both the *qki* gene and subsequent QKI expression (Ebersole *et al.*, 1996; Hardy *et al.*, 1996). QKI has been shown to selectively interact with 3´-untranslated region of the mRNA encoding for the structural protein MBP, resulting in post-transcriptional destabilization, mislocalization and misregulated splicing of the mRNA (Li *et al*., 2000; Zhang and Feng, 2001; Larocque *et al.*, 2002). These events compromise myelinogenesis in the CNS and qk^v/qk^v mice demonstrate severe hypomyelination with associated tremour (Sidman *et al.*, 1964). Other researchers have demonstrated that levels of QKI rapidly increase within the brain during a narrow developmental window with myelinogenesis at its most active, when the accumulation of both MBP and MBP mRNA is necessary (Zhang *et al*., 2003).

The *Src* family of protein tyrosine kinases (Src-PTKs) play an important role in signal transduction through mediating tyrosine phosphorylation in many RNA-binding proteins (Pype *et al.*, 1994; Wang *et al.*, 1995; Ostareck-Lederer *et al.*, 2002) and research has shown that the function of QKI, the RNA-binding protein mentioned above, is also regulated by the Src-PTKs through tyrosin phosphorylation (Zhang *et al*., 2003). Src-PTK modulates MBP mRNA binding by QKI in a negative way. Zhang *et al.* (2003), demonstrated that Src-PTKs

attenuated the interaction between QKI and MBP mRNA even though experimental conditions resulted in tyrosine phosphorylation of <50% of the input QKI.

Src-PTKs are also subject to regulation by upstream factors. One such a factor that regulates Src-PTK activity through selective inhibition is the protein phosphatase 2B (PP2B) also known as calcineurin (Salazar and Rozengurt, 2001), which is abundantly expressed in the brain (Kincaid, 1993). Calcineurin is dependent on Ca^{2+} for activation and in this way modulates Ca^{2+}-signalling (Allen and Sanders, 1995).

If all of the above is taken into account, the following hypothesis concerning the premature myelination seen in *Chapter 3* can be formulated:

Digoxin inhibited Na^+/K^+-ATPase, which increased $[Na^+]_i$. To compensate for the high levels of $[Na^+]_i$, the action of the Na^+/Ca^{2+}-exchanger is reversed. This extrudes Na^+ from the cell but results in the accumulation of Ca^{2+} within the cytosol. The increased levels of $[Ca^{2+}]_i$ induced Ca^{2+} release from intracellular stores such as the ER through Ca^{2+}-induced Ca^{2+} release (CICR). The sudden elevation in $[Ca^{2+}]_i$ activated calcineurin, which is Ca^{2+}-dependent. The Ca^{2+}/calcineurin complex inhibited the catalytic functioning of Src-PTKs that attenuate QKI binding to MBP mRNA. The result is premature onset of the "myelination window" during which Src-PTKs are inhibited and QKI binding helps in the effective stabilization, localization and splicing of MBP mRNA following transcription. This would lead to premature myelinogenesis. For a diagrammatic illustration of the proposed hypothesis see fig. 6.2.

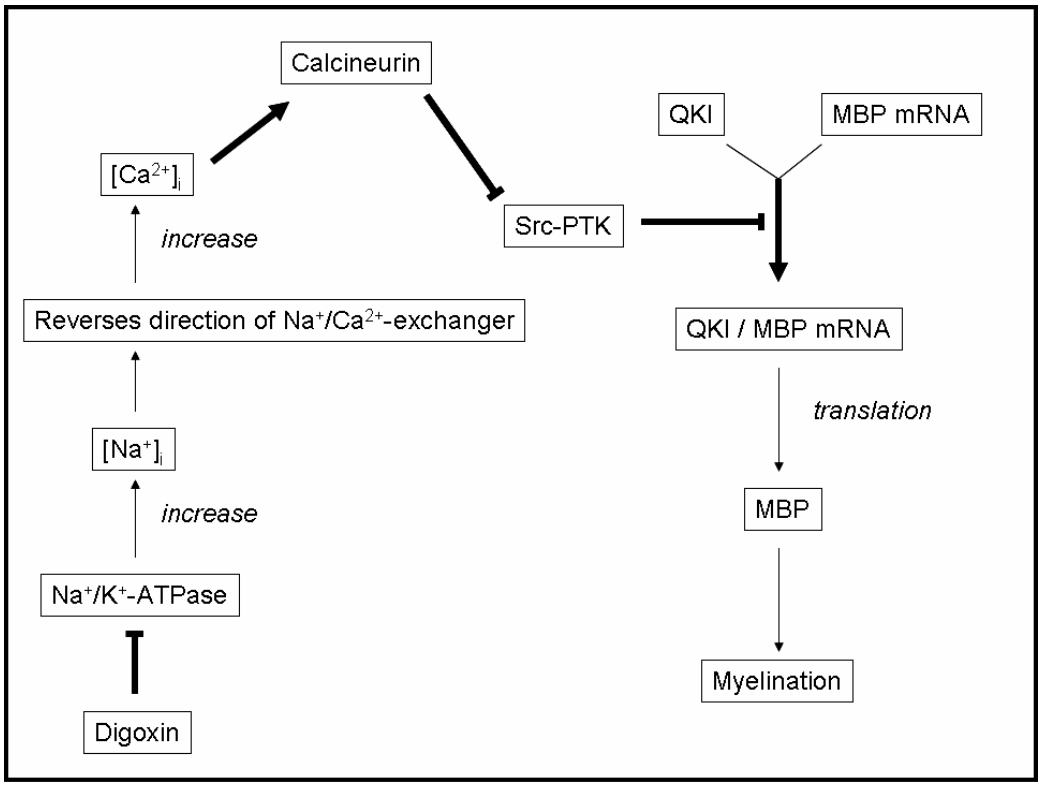

Fig. 6.2. Diagrammatic illustration of the proposed hypothesis on how Ca^{2+} influx can result in premature myelination in the chick embryo CNS. Dark arrows indicated upregulation or activation. Remaining dark lines represent inhibition. ***MBP*** **=** myelin basic protein; ***Src-PTK*** **=** *Src* family of protein tyrosine kinases; ***QKI*** **=** RNA binding protein.

6.2.2. Future research concerning premature myelinogenesis

In order to test whether calcineurin truly is the inhibitor of Src-PTK that results in premature myelination, the high dose experiment in *Chapter 3* can be repeated, but with the exception of adding a calcineurin inhibitor, such as either cyclosporine A or tachrolimus (Flechner, 2003). If it is determined that premature

myelination does still occur, then calcineurin inhibition of Src-PTK is not the primary cause of the premature myelination. This would immediately nullify the hypothesis given above and another inhibitor of Src-PTK should be searched for. The right arm of the diagram in fig. 6.2 has already been proven by Zhang *et al.* in 2003. Therefore, calcineurin forms the basis of the hypothesis suggested in fig. 6.2.

An alternative to calcineurin inhibition is that of inhibiting the Na^+/Ca^{2+}-exchanger, which reverses its action to extrude Na^+ from the cytosol but consequently increases cytosolic Ca^{2+}. Two such Na^+/Ca^{2+}-exahnger inhibitors available are KB-R7943 and SEA0400 (Myles, 2004). In a way this would also inhibit calcineurin by not allowing the increase of $[Ca^{2+}]_i$ via Na^+/Ca^{2+}-exchanger reversing its action. If one of these inhibitors is added to the experiment and premature myelination does not occur, it indicates that Ca^{2+} truly does play a role in the premature myelination seen. If premature myelination does occur it is indicative of either Ca^{2+} not playing a role and that myelinogenesis is induced by digoxin through some other mechanism, or that $[Ca^{2+}]_i$ increases through another mechanism.

To test if $[Ca^{2+}]_i$ and not digoxin, plays a role in the premature myelination, Melettin can be used to induce elevated $[Ca^{2+}]_i$ levels (Chen and Lin-Shiau, 1985). If premature myelination occurs, it can be hypothesized that the premature myelination is the result of high levels of Ca^{2+} in the cytosol.

6.3. SEROTONIN

6.3.1. Hypothesis concerning digoxin's effect on brain serotonin levels

Serotonin or 5-hydroxytryptamine is one of the earliest developing neurotransmitter systems, as early as 5 weeks of gestation (Sundstrom *et al.*,

1993), in the mammalian brain (Aitken and Tork, 1988; Lauder, 1990). Thus, serotonin develops early enough, and is widespread enough through the brain that it can influence maturation of many other cells in the brain. Digoxin can influence serotonin production and its effect on the developing brain in several different ways, which will be discussed in the following paragraphs.

Serotonin functions in a negative feedback manner. When serotonin innervation in the brain exceeds a certain threshold level, serotonin terminals start deteriorating. In autistic children and children with hypertryptophanemia it was speculated that an endogenous digoxin-like immunoreactive factor (DLIF), causes a tip in the balance of amino acids entering the brain in such a way that more tryptophan (the precursor for serotonin) enters the brain and elevated levels of DLIF may increase the child's chances of developing autism (Hoshino, 1986).

The initial and rate-limiting enzyme in the biosynthesis of serotonin is known as tryptophan hydroxylase (TH). TH activation is Ca^{2+} dependent and can be activated by ATP-Mg^{2+}. The reaction that activates the enzyme is a phosphorylation reaction and the phosphate ion required is provided by ATP. Ca^{2+} increases the activating effect that ATP-Mg^{2+} has on the enzyme and it is strongly suggested in the literature that the activation of TH is achieved by a Ca^{2+}-dependent protein kinase (Kuhn *et al.*, 1978; Hamon *et al.*, 1978). From the results obtained in this dissertation, it is now known that digoxin exposure in chick embryo neurons increases Ca^{2+} in the cytosol and that ATP will be depleted at concentrations high enough to compromise mitochondrial function. From this it could be speculate that low concentrations of digoxin, which causes increased $[Ca^{2+}]_i$ without compromising mitochondrial function, will increase serotonin production through activation of TH. On the other hand, serotonin production will cease once cellular ATP stores are depleted, as is the case with neuronal exposure to high concentrations of digoxin that irreversibly damage mitochondria. Therefore, when observing a wide range of digoxin concentrations,

a slight to moderate increase in serotonin production is expected and as the concentrations increase, a decrease and complete cessation of serotonin production could possibly follow.

Another pathway through which digoxin can affect serotonin levels present in the brain is through the enzyme monoamine oxidase A (MAO-A). Under physiological conditions, extracellular serotonin build-up is degraded by MAO-A through the catabolism of serotonin (Leonardi and Azmitia, 1994). Recently, Kosenko *et al.* (2003), demonstrated that Ca^{2+} increases the activity of MAO-A but not MAO-B (degrades dopamine) both *in vitro* and *in vivo*. From this it could again be deducted that digoxin should have an increasing effect on serotonin levels present in the brain because Ca^{2+} inhibits MAO-A function and digoxin increases cytosolic Ca^{2+} levels.

Therefore, the following hypothesis is suggested concerning digoxin's effect on brain serotonin levels:

In vivo or *in ovo* exposure to digoxin will cause an increase in the embryonal/foetal brain in three ways. First, digoxin tips the balance of amino acids entering the brain in such a way that more tryptophan enters the brain and will in this way elevate brain serotonin levels. Second, more tryptophan will be converted to serotonin faster because the activity of TH, the rate-limiting step in serotonin biosynthesis, is increased. Thirdly, digoxin increases $[Ca^{2+}]_i$, which inhibits MAO-A. MAO-A can therefore not degrade serotonin and levels of extracellular serotonin rise. This hypothesis is graphically illustrated in fig. 6.3. It must be noted that the entire hypothesis only applies to digoxin concentrations where mitochondrial function remains intact.

6.3.2. Future research concerning digoxin's effect on brain serotonin levels

Previous researchers have used high performance liquid chromatography (HPLC) as a means of measuring the serotonin content in brain tissue. This technique has been used in various animal models including eels and chickens (Sebert *et al.*, 1987; Siuciak *et al.*, 1992). This technique would also be able to detect the amount of tryptophan present in brain tissue. It would be best to determine the effect that digoxin would have on brain serotonin levels in an *in ovo* model to better appreciate the effect on serotonin in an organism and not *in vitro*, which could show differing results from those obtained with the organism intact. One could repeat the low- and high dose arms of the experiment performed in *Chapter 3*. This would give an indication of whether low concentrations of digoxin will increase brain serotonin levels as opposed to the expected decrease in brain serotonin levels following exposure to high concentrations of digoxin.

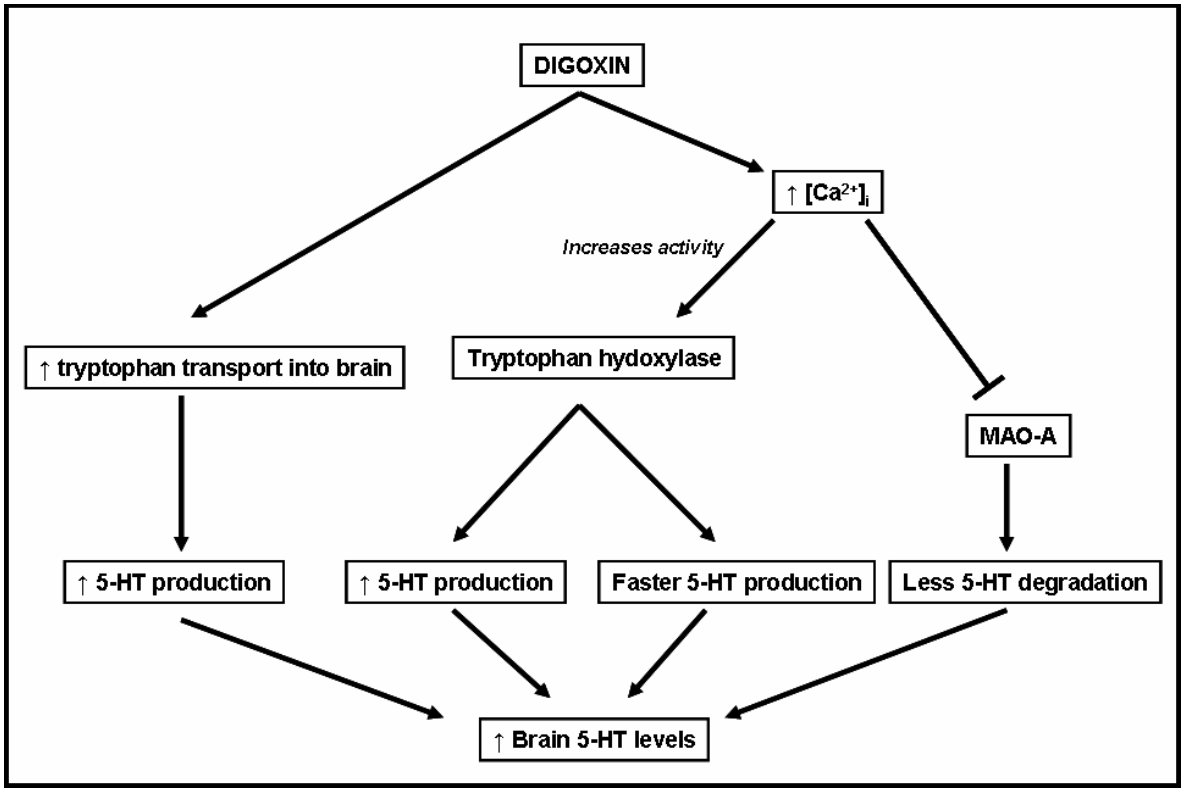

Fig. 6.3. Diagrammatic illustration pertaining to the hypothesis on how digoxin could increase brain serotonin levels. It must be noted that the entire hypothesis only applies to digoxin concentrations where mitochondrial function remains intact. ***MAO-A*** **=** monoamine oxidase A; ***5-HT*** **=** serotonin (5-hydroxytryptophan).

If it is determined that brain serotonin does increase with digoxin exposure, melettin could perhaps be utilized and possibly also a Na^+/Ca^{2+}-exchanger inhibitor. Replacing digoxin with melettin allows the researcher to assess the effect of digoxin on tryptophan transport into the brain, which could be tested with HPLC. From the literature, it is expected that an increase in tryptophan transport into the brain should not occur.

The Na^+/Ca^{2+}-exchanger inhibitor, SEA0400, can be used to halt the increase in $[Ca^{2+}]_i$ and this could then be used to examine the final parts of the hypothesis illustrated in fig. 6.3. If brain serotonin is not increased in the experimental group receiving the SEA0400, it would indicate that the mechanism through which

digoxin would increase brain serotonin levels is via increased Ca^{2+} affecting both TH and MAO-A.

6.4. IN SUMMARY

This study has shown that digoxin has a profound effect on neuronal development, viability and cellular physiology at high concentrations. Most of the effects that digoxin exerts on neuronal tissue is by means of increasing $[Ca^{2+}]_i$. Concerning neuronal viability, this drug induces apoptosis at low concentrations through inducing MPT and necrosis at high concentrations through compromising mitochondrial function and energy metabolism.

An unexpected result was that of the premature myelinogenesis induced by high concentrations of digoxin. It is not clear what the cause of the myelinogenesis was and further research is warranted. It could give researchers insight into myelinogenesis, which could possibly later be applied in neurodegenerative disorders such as multiple sclerosis and spinal cord injuries to promote myelinogenesis and nerve regrowth. Probably the best area to start investigating would be that of protein synthesis through proteomics to determine what proteins are being mass produced. This would indicate where either digoxin or Ca^{2+} is playing a role in order to result in this rapid myelinogenesis. The role of digoxin in serotonin production and serotonin levels in the brain is not known in the literature. This should be investigated further as this might associate with the premature myelinogenesis that was observed.

Chapter 7:

References.

Agar A, Li S, Agarwal N, Coroneo MT, Hill MA. (2006) Retinal ganglion cell line apoptosis induced by hydrostatic pressure. Brain Research 1086: 191-200.

Ahlbom E, Grandison L, Bonfoco E, Zhivotovsky B, Ceccatelli S. (1999) Androgen treatment of neonatal rats decreases susceptibility of cerebellar granule neurons to oxidative stress *in vitro.* European Journal of Neuroscience 11 (4): 1285-1291.

Aitken AR, Tork I. (1988) Early development of serotonin-containing neurons and pathways as seen in wholemount preparations of the fetal rat brain. The Journal of Comparative Neurology 274(1): 32-47.

Allen GJ, Sanders D. (1995) Calcineurin, a type 2B protein phosphatase, modulates the Ca^{2+}-permeable slow vacuolar ion channel of stomatal guard cells. Plant Cell 7(9): 1473-1483.

Asaba H, Hosoya K, Takanaga H, Ohtsuki S, Tamura E, Takizawa T, et al. (2000) Blood-brain barrier is involved in the efflux transport of a neuroactive steroid, dehydroepiandrosterone sulfate, via organic anion transporting polypeptide 2. Journal of Neurochemistry 75: 1907-1916.

Bauer M, Kristensen BM, Meyer M, Gasser T, Widmer HR, Zimmer, J, Ueffing M. (2006) Toxic effects of lipid-mediated gene transfer in ventral mesencephalic explant cultures. Basic and Clinical Pharmacology and Toxicology 98 (4): 395-400.

Bernardi P. (1999) Mitochondrial transport of cations: channels, exchangers, and permeability transition. Physiological Reviews 79: 1127-55.

Berridge MJ, Bootman MD, Roderick HL. (2003) Calcium signaling: dynamics, homeostasis and remodelling. Nature Reviews Molecular Cell Biology 4: 517-29.

Bizzozero OA, Bixler HA, Davis JD, Espinosa A, Messier AM. (2001) Chemical deacylation reduces the adhesive properties of proteolipid protein and leads to decompaction of the myelin sheath. Journal of Neurochemistry 76: 1129-1141.

Black D, Bird MA, Samson CM, Lyman S, Lange PA, Schrum LW, Qian T, Lemasters JJ, Brenner DA, Rippe RA, Behrns KE. (2004) Primary cirrhotic hepatocytes resist TGFbeta-induced apoptosis through a ROS-dependent mechanism. Journal of Hepatology 40: 942-951.

Blanco G, Mercer RW. (1998) Isozymes of the Na^+,K^+-ATPase: heterogeneity in structure, diversity in function. American Journal of Physiology 275: F633-F650.

Blasi JMV, Cena V, Gonzalez-Garcia C, Marsal J, Solsona C. (1998) Ouabain induces acetylcholine release from pure cholinergic synaptosomes independently of extracellular calcium concentrations. Neurochem Res 13: 1035-1041.

Brostrom CO, Bocckino SB, Brostrom MA. (1983) Identification of a Ca^{2+} requirement for protein synthesis in eukaryotic cells. Journal of Biological Chemistry 258(23): 14390-14399.

Campagnoni AT, Macklin WB. (1988) Cellular and molecular aspects of myelin protein gene expression. Mol Neurobiol 2: 41-89.

Carafoli E, Santella L, Branca D, Brini M. (2001) Generation, control, and processing of cellular calcium signals. Critical Reviews in Biochemistry and Molecular Biology 36: 107-260.

Castilla R, Gonzalez R, Fouad D, Fraga E, Muntane J. (2004) Dual effect of ethanol on cell death in primary culture of human and rat hepatocytes. Alcohol and Alcoholism 39(4): 290-296.

CellProbe™ Reagents: An Introduction. (2001) Retrieved from [http://webdev.beckman.com/Coulter/Cytometry/CellProbe-Reagents(copy)/cp-index.asp] on 13 February 2007.

Chen CC, Lin-Shiau SY. (1985) Mode of inhibitory action of Melettin on Na+-K+-ATPase activity of the rat synaptic membrane. Biochemical Pharmacology 34(13): 2335-41.

Cheng W, Quimby FW, Lei XG. (2003) Impacts of glutathione peroxidase-1 knockout on the protection by injected selenium against the pro-oxidant-induced liver aponecrosis and signaling in selenium deficient mice. Free Radical Biology and Medicine 34(7): 918–927.

Chin KV, Cade C, Brostrom CO, Galuska EM, Brostrom MA. (1987) Calcium-dependent regulation of protein synthesis at translational initiation in eukaryotic cells. Journal of Biological Chemistry 262(34): 16509-16514.

Christian HA. (1922) Digitalis effects in chronic cardiac cases with regular rhythm in contrast to auricular fibrillation. Medical Clinics of North America 5: 1173-1190.

Chubakov AR, Gromova EA, Konovalov GV, Sarkisova EF, Chumasov EI. (1986) The effects of serotonin on the morphofunctional development of rat cerebral neocortex in tissue culture. Brain Research 369: 285 297.

Chubakov AR, Tsyganova VG, Sarkisova EF. (1993) The stimulating influence of the raphe nuclei on the morphofunctional development of the hippocampus during their combined cultivation. Neuroscience and Behavioral Physiology 23: 271-276.

Crompton M. (1999) The mitochondrial permeability transition pore and its role in cell death. Biochemical Journal 341: 233-49.

Datta P, Dasgupta A. (2004) Interference of Endogenous Digoxin-Like Immunoreactive factors in serum digoxin measurement is minimized in a new turbidimetric digoxin immunoassay on ADVIA 1650 Analyzer. Therapeutic Drug Moinitoring 1(24): 85-89.

The Digitalis Investigation Group (DIG). (1996) Rationale, design, implementation, and baseline characteristics of patients in the DIG trial: A large, simple, long-term trial to evaluate the effect of digitalis on mortality in heart failure. Controlled Clinical Trials 17: 77-97.

Dong Z, Saikumar P, Weinberg JM, Venkatachalam MA. (2006) Calcium in cell injury and death. Annual Review of Pathology: Mechanisms of Disease 1: 405-434.

Duchen MR. (2000) Mitochondria and calcium: from cell signaling to cell death. Journal of Physiology 529: 57-68.

Ebersole TA, Chen Q, Justice M J, Artzt K. (1996) The quaking gene product necessary in embryogenesis and myelination combines features of RNA binding and signal transduction proteins. Nature Genetics 12: 260-265.

Edelstein CL, Ling H, Schrier RW. (1997) The nature of renal cell injury. Kidney International 51: 1341-51.

Eichhorn EJ, Gheorghiade M. (2002) Digoxin. Progress in Cardiovascular Diseases 4(44): 251-266.

Elliott SJ, Doan TN, Henschke PN. (1995) Reductant substrate for glutathione peroxidase modulates oxidant inhibition of Ca2+ signaling in endothelial cells. American Journal of Physiology: Heart and Circulatory Physiology 268: 278-287.

Fineman RM, Schoenwolf GC. (1987) Animal model: dysmorphogenesis and death in a chicken embryo model. American Jorunal of Mecial Genetics 27(3): 543-52.

Flechner SM. (2003) Minimizing calcineurin inhibitor drugs in renal transplantation. Transplantation Proceedings 35: 118S-121S.

Geering, K, Beggah, A, Good P, Girardet S, Roy S, Schaer D, Jaunin P. (1996) Oligomerization and maturation of Na,K-ATPase: functional interaction of the cytoplasmic NH_2 terminus of the β-subunit with the α-subunit. Journal of Cell Biology 133: 1193-1204.

Gerbi A, Ze´rouga M, Maixent JM, Debray M, Durand G, Bourre JM. (1999) Diet deficient in alpha-linolenic acid alters fatty acid composition and enzymatic properties of Na+, K+-ATPase isoenzymes of brain membranes in the adult rat. Journal of Nutritional Biochemistry 10: 230-236.

Goldberg A. (1989) A shared view of the world. International Journal of Psycho-Analysis 70(1): 16-20.

Goodlett CR, Horn KH. (2001) Mechanism of alcohol-induced damage to the developing nervous system. Alcohol Research and Health, Fall issue.

Gvozdjan DM, Bowden ET, Wellstein A. (2004) A novel chicken embryo model for the investigation of drugs with antimetastatic properties. Clinical Pharmacology and Therapeutics 75: 60.

Hambarchian N, Brixius K, Lu R, Müller-Ehmsen J, Schwinger RHG. (2004) Ouabain increases myofibrillar Ca^{2+} sensitivity but does not influence the Ca^{2+} release in human skinned fibres. European Journal of Pharmacology 492: 225-231.

Hamon M, Bourgoin S, Hery F, Simonnet G. (1978) Molecular Pharmacology 14: 99-110.

Hardy RJ, Loushin CL, Friedrich VL, Chen Q, Ebersole TA, Lazzarini RA, Artzt K. (1996) Neural cell type-specific expression of QKI proteins is altered in quakingviable mutant mice. Journal of Neuroscience 16: 7941-7949.

Haupert GT. (1989). Sodium pump regulation by endogenous inhibition. Topics in Membrane Transport 34: 345-348.

Herrera VLM, Emanuel JR, Ruiz-Opazo N, Levenson R, Nadal-Ginard B. (1987) Three differentially expressed Na,K-ATPase α-subunit isoforms: structural and functional implications. Journal of Cell Biology 105: 1855-1865.

Hisaka A, Kasamatu S, Takenaga N. (1990) Absorption of a novel prodrug of DOPA. Drug-Metabolism Disposal 18: 621-625.

Hoshino Y, Yamamoto T, Kaneko M, Kumashiro H. (1986) Plasma free tryptophan concentration in autistic children. Brain Development 8(4): 424-427.

Huang J, May MJ. (2006) Ascorbic acid protects SH-SY5Y neuroblastoma cells from apoptosis and death induced by β-amyloid. Brain Research 1097: 52-58.

Huang YT, Chueh S, Teng C, Guh J. (2004) Investigation of ouabain-induced anticancer effect in human androgen-independent prostate cancer PC-3 cells. Biochemical Pharmacology 67: 727-733.

Ichinose M, Yonemochi H, Sato T, Saikawa T. (2003) Diazoxide triggers cardioprotection against apoptosis induced by oxidative stress. American Journal of Physiology: Heart and Circulatory Physiology 284: H2235–H2241.

Iwaki M, Kumagai S, Akamatsu Y, Kitagawa T. (1993) Aflatoxin B[1]-binding proteins in primary cultured hepatocytes of chicken embryo : studies in vivo and in vitro. Biochimica et biophysica acta 1225(1): 83-88.

James PR. (2004) A review of peripartum cardiomyopathy. International Journal of Clinical Practice 58(4): 363-365.

Jung C, Higgins CM, Xu Z. (2000) Measuring the quantity and activity of mitochondrial electron transport chain complexes in tissues of central nervous system using blue native polyacrylamide gel electrophoresis. Analytical Biochemistry 286(2):214-23.

Jung KH, Chu K, Lee ST, Kang L, Kim SU, Kim M, Roh JK. (2006) G-CSF protects human cerebral hybrid neurons against in vitro ischemia. Neuroscience Letters 394: 168-173.

Kang W, Weiss M. (2002) Digoxin Uptake, Receptor Heterogeneity, and Inotropic Response in the Isolated Rat Heart: A Comprehensive Kinetic Model. Journal of Pharmacology and Experimental Therapeutics 302(2): 577-583.

Kent MH, Huang BS, Van Huysse JW, Leenen FHH. (2004) Brain Na+,K+-ATPase isozyme activity and protein expression in ouabain-induced hypertension. Brain Research 1018: 171-180.

Kincaid RL. (1993). Calmodulin-dependent protein phosphatases from microorganisms to man: a study in structural convertism and biological diversity. Adv Second Messenger Phosphoprotein Research 27: 1-23.

Kosenko EA, Venediktova NI, Kamanskii IuG. (2003) Calcium and ammonia stimulate monoamine oxidase A activity in brain mitochondria. Izv Akad Nauk Ser Biol 5: 542-6.

Krapp M, Baschat AA, Gembruch U, Geipel A, Germer U. (2002) Flecainide in the intrauterine treatment of fetal supraventricular tachycardia. Ultrasound in Obstetrics and Gynecology 19: 158-164.

Kuhn DM, Vogel RL, Lovenberg W. (1978) Biochemical and Biophysical Research Communications 82: 759-766.

Kurup RK, Kurup PA. (2002) Hypothalamic digoxin related membrane Na+–K+ ATPase inhibition and familial basal ganglia calcification. Neuroscience Research 42: 35-44.

Kurup RK, Kurup PA. (2003) Hypothalamic digoxin, hemispherical chemical dominance, and addictive behaviour. International Journal of Neuroscience 113: 279-289.

Larocque D, Pilotte J, Chen T, Cloutier F, et al. (2002) Nuclear retention of MBP mRNAs in the quaking viable mice. Neuron 36: 815-829.

Lauder JM. (1990) Ontogeny of the serotonergic system in the rat: serotonin as a developmental signal. Annals of the New York Academy of Sciences 600: 297-313.

Lemarie A, Morzadec C, Me´rino D, Micheau O, Fardel O, Vernhet L. (2006) Arsenic trioxide induces apoptosis of human monocytes during macrophagic differentiation through nuclear factorβ-related survival pathway down-regulation. Journal of Pharmacology and Experimental Therapeutics 316: 304-314.

Lemasters JJ, Nieminen AL, Qian T,Trost LC, Elmore SP, *et al*. (1998) The mitochondrial permeability transition in cell death: a common mechanism in necrosis, apoptosis and autophagy. Biochimica et Biophysica Acta 1366: 177-96.

Leonardi ET, Azmitia EC. (1994) MDMA (ecstasy) inhibition of MAO type A and type B: comparisons with fenfluramine and fluoxetine (Prozac). Neuropsychopharmacology 10(4): 231-8.

Li Z, Zhang Y, Li D, Feng Y. (2000) Destabilization and mislocalization of myelin basic protein mRNAs in quaking dysmyelination lacking the QKI RNA-binding proteins. Journal of Neuroscience 20: 4944-4953.

Liu X, Van Vleet T, Schnellmann RG. (2004) The role of calpain in oncotic cell death. Annual Review of Pharmacology and Toxicology 44: 349-70.

Luyten GPM, Mooy CM, De Jong PTVM, Hoogeveen AT, Luider TM. (1993) A chicken embryo model to study the growth of human uveal melanoma. Biochemical and Biophysical Research Communications 192(1): 22-29.

Martin-Vasallo P, Dackowski W, Emanuel JR, Levenson R. (1989) Identification of a putative isoform of the Na,K-ATPase β-subunit: primary structure and tissue-specific expression. Journal of Biological Chemistry 264: 4613-4618.

Marvin HM. (1927) Digitalis and diuretics in heart failure with regular rhythm, with special reference to importance of etiologic classification of heart disease. Journal of Clinical Investigation 3: 521-539.

Marx J, Pretorius E, Espag WJ, Bester MJ. (2005) *Urginea sanguinea*: medicinal wonder or death in disguise? Environmental Toxicology and Pharmacology 20: 26-34.

Marx J. (2005) Investigation of the cytotoxic potential of aqueous extracts of *Dicerocaryum* zanguebarium and Urginea sanguinea *in vitro*. University of Pretoria MSc Thesis.

Meissner G. (2004) Molecular regulation of cardiac ryanodine receptor ion channel. Cell Calcium 35: 621-28.

Mobasheri A, Avila J, Cozar-Castellano I, Brownleader MD, Trevan M, Francis MJO, Lamb JF, Martin-Vasallo P. (2000) Na^+,K^+- ATPase isozyme diversity; comparative biochemistry and physiological implications of novel functional interactions. Bioscience Reports 20: 51-91.

Meyer ME, Cooper JR. (1981) Correlation between Na+,K+-ATPase activity and acetylcholine release in rat cortical synaptosomes. Journal of Neurochemistry 36: 467-475.

Mufson RA, Laskin JD, Fisher PB, Weinstein JB. (1979) Melettin shares certain cellular effects with phorbol ester tumour promoters. Nature 280: 72-74.

Myles HA. (2004) Na^+/Ca^{2+} Exchange Inhibitors: Potential Drugs to Mitigate the Severity of Ischemic Injury. Molecular Pharmacology 66: 8-10.

Neuhofer W, Woo SK, Na KY, Nbein RG, Park WK, Nahm O, Beck FX, Kwon HM. (2002) Regulation of TonEBP transcriptional activator in MDCK cells following changes in ambient tonicity. American Journal of Physiology: Cell Physiology 283: C1604–C1611.

Norton JD, Atherton GT. (1998) Coupling of Cell Growth Control and Apoptosis Functions of Id Proteins. Molecular and Cellular Biology 18(4): 2371-2381.

O'Rhailly R, Müller F. (1987) Developmental stages in human embryos, publication no. 637. Washington: Carnegie Institute.

O'Rahilly R, Müller F. (1999) The embryonic human brain. An atlas of developmental stages, 2nd ed. Wiley-Liss.

Orlowski J, Lingrel JB. (1988) Tissue-specific and developmental regulation of rat Na,K-ATPase catalytic α-isoform and β-subunit mRNAs. Journal of Biological Chemistry 263: 10436-10442.

Ostareck-Lederer A, Ostareck DH, Cans C, Neubauer G, Bomsztyk K, Superti-Furga G, Hentze MW. (2002) c-Src mediated phosphorylation of hnRNP K drives translational activation of specifically silenced mRNAs. Molecular Cell Biology 22: 4535-4543.

Patterson RL, Boehning D, Snyder SH. (2004) Inositol 1,4,5-trisphosphate receptors as signal integrators. Annual Review of Biochemistry 73: 437-65.

Paszkiewicz-Gadek A, Chlabicz J, Galasinski W. (1988) The influence of selected potential oncostatics of plant origin on the protein biosynthesis in vitro. Polish Journal of Pharmacology and Pharmaceutics 40(2): 183-90.

Pretorius E, Bornman MS. (2005) Calcium-mediated aponecrosis plays a central role in the pathogenesis of estrogenic chemical-induced neurotoxicity. Medical Hypotheses 65: 893-904.

Pozzo N, Miller LD, Mahanty NK, Connor JA, Landis DM. (1994) Spontaneous pyramidal cell death in organotypic slice cultures from rat hippocampus is prevented by glutamate receptor antagonists. Neuroscience 63: 471-487.

Pype S, Slegers H, Moens L, Merlevede W, Goris J. (1994) Src-PTKs regulate mRNA metabolism via QKI protein Tyrosine phosphorylation of a M(r) 38 000 A/B-type hnRNP protein selectively modulates its RNA binding. Journal of Biological Chemistry 269: 31457-31465.

Qasqas SA, McPherson C, Frishman WH, Elkayam U. (2004) Cardiovascular pharmacotherapeutic consideration during pregnancy and lactation. Cardiology in review 12: 201-221.

Ravikumar A, Jyothi A, Kurup PA. (2001). ^{14}C-acetate incorporation into digoxin in rat brain and effect of digoxin administration. Indian Journal of Experimental Biology 3: 420-426.

Reißenweber J, Poess J, David E. (2005) Sensitivity of children to EMF exposure – do elevated susceptibilities to high-frequency mobile communication fields exist during discrete developmental phases? Forschungsgemeinschaft Funk G14515 Issue 22.

Reinés A, Peña C, Rodríguez de Lores Arnaiz G. (2001) [^{3}H]Dizocilpine binding to N-methyl-D-aspartate (NMDA) receptor is modulated by an endogenous Na+/K+-ATPase inhibitor. Comparison with ouabain. Neurochemistry International 39: 301-310.

Roche Applied Sciences, Apoptosis, Cell death and Cell proliferation [Manual], 3rd ed. Retrieved April 18, 2007 from https://www.roche-appliedsciences.com/sis/apoptosis/docs/manual_apoptosis.pdf.

Roots B. (1995) The evolution of myelinating cells, Neuron–Glia Interrelations during Phylogeny. I. Phylogeny and Ontogeny of Glial Cells. Totowa: Humana Press Inc.

Sadler TW. (2000) Langman's medical embryology. 8th ed. Philadelphia: Lippincott Wlliams and Wilkins.

Salazar EP, Rozengurt E. (2001) Src family kinases are required for integrin mediated but not for G protein-coupled receptor stimulation of focal adhesion kinase autophosphorylation at Tyr-397. Journal of Biological Chemistry 276: 17788-17795.

Salthouse TN. (1964) Luxol-fast blue G as a myelin stain. Stain Technology 39: 1-8.

Saotome K, Morita H, Umeda M. (1989) Cytotoxicity test with simplified crystal violet staining method using microtitre plates and its application to injection drugs. Toxicology *in Vitro* 3: 317-321.

Satoh E, Nakazato Y. (1989) [^{3}H]Acetylcholine release and the change in cytosolic free calcium level induced by high K^{+} and ouabain in rat synaptosomes. Neuroscience Letters 107: 284-288.

Scarborough GA. (1999) Structure and function of the P-type ATPases. Current Opinions in Cell Biology 11: 517-522.

Schloss P, Williams DC. (1998) The serotonin transporter: a primary target for antidepressant drugs. Journal of Psychopharmacology 12(2): 115-21.

Sebert P, Barthelemy L, Caroff J. (1987) Serotonin levels in fish brain: Effects of hydrostatic pressure and water temperature. Cellular and Molecular Life Sciences 41(11): 1429-1430.

Shull GE, Greeb J, Lingrel JB. (1986) Molecular cloning of three distinct forms of the Na^+,K^+- ATPase α-subunit from rat brain. Biochemistry 25(a): 8125-8132.

Sidman RL, Dickie MM, Appel SH. (1964) Mutant mice (Quaking and Jimpy) with deficient myelination in the central nervous system. Science 144: 309-311.

Siuciak J, Gamache PH, Dubocovich ML. (1992) Monoamines and Their Precursors and Metabolites in the Chicken Brain, Pineal, and Retina: Regional Distribution and Day/Night Variations Journal of Neurochemistry 58(2): 722.

Smith TW, Haber E. (1970) Digoxin intoxication: The relationship of clinical presentation to serum digoxin concentration. Journal of Clinical Investigation 49: 2377-2386.

Sokoloff L. (1993) Sites and mechanisms of function-related changes in energy metabolism in the nervous system. Developmental Neuroscience 15: 194-206.

Soyka LF. (1975) Digoxin: placental transfer, effects on the fetus, and therapeutic use in the newborn. Clinical Perinatology 2(1): 23-35.

Sundstrom E, Kolare S, Souverbie F, Samuelsson EB, Pschera H, Lunell NO, Seiger A. (1993) Neurochemical differentiation of human bulbospinal monoaminergic neurons during the first trimester. Developmental Brain Research 75(1): 1-12.

Sweadner KJ. (1989) Isozymes of the Na^+/K^+-ATPase. Biochimica et Biophysica Acta 988: 185-220.

Sweadner KJ. (1992) Overlapping and diverse distribution of the Na^+,K^+- ATPase isozymes in neurons and glia. Canadian Journal of Physiology and Pharmacology 70: 255-259.

Stojanonic T, Djuricic BM, Mursulja BB. (1980) The effect of physostigmine on (Na^+/K^+)-ATPase activity in different rat brain regions. Experientia 36: 1348-1350.

Tieffenberg J, Vogel L, Kretschmer RR, Padnos D, Gotoff SP. (1978) Chicken embryo model for type III group B beta-hemolytic streptococcal septicemia. Infection and Immunity 19(2): 481-485.

Tuschl H, Schwab CE. (2004) Flow cytometric methods used as screening tests for basal toxicity of chemicals. Toxicology in Vitro 18: 483-491.

Van der Merwe CF, Coetzee J. (1992) Quetol 651 for general use: revised formulation. Proceedings of electron microscopic society of South Africa 22: 31-32.

Vanderklish PW, Bahr BA. (2000) The pathogenic activation of calpain: a marker and mediator of cellular toxicity and disease states. International Journal of Experimental Pathology 81: 323-39.

Vigil EL, Steere RL, Wergin WP Christiansen MN. (1984) Tissue preparation and fine structure of the radicle apex from cotton seeds. American Journal of Botany 71: 645-659.

Volkmann KR and Morgan HR. (1974) Virus Production and Release, Cell Longevity, and Cloning Efficiency of Chicken Embryo Fibroblasts Infected with Rous Sarcoma Virus. Infection and Immunity 10(4): 834-843.

Wang H, Yuan WQ, Lu ZR. (2000) Differential regulation of the sodium pump alpha-subunit isoform gene by ouabain and digoxin in tissues of rats. Hypertension Research 23: S55-S60.

Wang LL, Richard S, Shaw AS. (1995) P62 association with RNA is regulated by tyrosine phosphorylation. Journal of Biological Chemistry270: 2010-2013.

Withering W. (1941) An account of the foxglove and some of its medical uses, with practical remarks on dropsy, and other diseases, in Willins FA, Keys TE (eds): Classics of Cardiology, vol I. New York, Henry Schuman, Dover Publications, pp 231-52.

Whitley D, Goldberg SP, Jordan WD. (1999) Heat shock proteins: A review of the molecular chaperones. Journal of Vascular Surgery 29: 748-51.

Yeh CJ, Hsi BL, Faulk WP. (1981) Propidium iodide as a nuclear marker in immunofluorescence. II. Use with cellular identification and viability studies. Journal of Immunological Methods 43(3): 269-275.

Yusuf S. (1993) Clinical experience in protecting the failing heart. Clinical Cardiology 16: 27-29.

Zhang Y, Feng Y (2001) Distinct molecular mechanisms lead to diminished myelin basic protein and 2′,3′-cyclic nucleotide 3′- phosphodiesterase in qk(v) dysmyelination. Journal of Neurochemistry 77: 165-172.

Zhang Y, Lu Z, Ku L, Chen Y, Wang H, Feng Y. (2003) Tyrosine phosphorylation of QKI mediates developmental signals to regulate mRNA metabolism. The European Molecular Biology Organization Journal 22 (8): 1801-1810.